Author Summary

Asthma is the most common chronic disorder in children, and asthma exacerbation is an important cause of childhood morbidity and hospitalization. Here, taking advantage of recent technological advances in human genetics, we performed a genome-wide association study and follow-up validation studies to identify genetic variants for asthma. By examining 6,428 Asians, we found rs987870 and *HLA-DPA1*0201/DPB1*0901* were associated with pediatric asthma. The association signal was stretched in the region of *HLA-DPB2*, collagen, type XI, alpha 2 (*COL11A2*), and Retinoid X receptor beta (*RXRB*), but strong linkage disequilibrium in this region made it difficult to specifically identify causative variants. Interestingly, the SNP (or the HLA-DP allele) associated with pediatric asthma (Th-2 type immune diseases) in the present study confers protection against Th-1 type immune diseases, such as type 1 diabetes and rheumatoid arthritis. Therefore, the association results obtained in the present study could partially explain the inverse relationship between asthma and Th-1 type immune diseases and may lead to better understanding of Th-1/Th-2 immune diseases.

RAD50 and *IL5* on chromosome 5q (OR = 1.64, $P = 3.0 \times 10^{-7}$) and *HLA-DR/DQ* (OR = 0.68, $P = 9.6 \times 10^{-6}$), but they did not include a replication dataset [7]. Recently, Moffatt *et al.* conducted a large-scale GWAS in Caucasian populations and identified 6 loci (*IL18R1*, *HLA-DQ*, *IL33*, *SMAD3*, *GSDMB/GSDMA*, and *IL2RB*) associated with asthma [8].

In the present study, we conducted the first GWAS in Asian population for pediatric asthma by using Illumina HumanHap550/610-Quad BeadChip (Illumina, San Diego, USA).

Results

GWAS analysis

The GWAS flow chart is shown in Figure 1. We analyzed 450,326 SNPs in 938 cases and 2,376 controls, using standard quality control practices (Table S1). The genotypes in cases and controls were compared using the Cochran–Armitage trend test (Figure 2). There was only minor inflation of the genome-wide statistical results owing to population stratification (genomic control (λ_{GC}) = 1.048; Figure 3). Five SNPs (rs3019885, rs987870, rs2281389, rs2064478, and rs3117230) showed strong association with pediatric asthma with $P < 1 \times 10^{-8}$. Of these, rs2064478 and rs3117230 were in complete linkage disequilibrium (LD) ($r^2 = 1$) with rs2281389. In order to validate the results of the GWAS, we tested the remaining 3 SNPs (rs3019885, rs987870, and rs2281389) in 2 independent replication cohorts comprising Asians (Japanese and Koreans), considering $P < 0.05$ as significant replication.

Of these 3 SNPs, significant associations were noted at rs987870 in both cohorts (Table 1). To merge the findings of these studies, we conducted meta-analysis with a fixed-effects model by using the Mantel–Haenszel method. As shown in Table 1, the Mantel–Haenszel P value of 2.3×10^{-10} was noted for rs987870 (OR = 1.40, confidence interval (CI) = 1.26–1.55).

HLA-DP association with pediatric asthma

The rs987870 is located between *HLA-DPA1* and *HLA-DPB1*. Genotype imputation using MACH [9] revealed association between asthma and the SNPs that were in strong LD with rs987870 (Figure 4, Table S2). Moreover, rs987870 C allele was in complete LD with *DPA1*0201* ($r^2 = 1$). We determined *HLA-DPA1* genotypes by using direct sequencing and MACH imputation of the data from 1135 cases and 2376 controls and found that *DPA1*0201* was strongly associated with pediatric asthma ($P = 5.2 \times 10^{-10}$, OR = 1.52, Table 2). Then, we determined the *HLA-DPB1* genotypes in 1135 cases and 2296 controls and found that *DPB1*0901* was associated with pediatric asthma ($P = 2.0 \times 10^{-7}$, OR = 1.49, Table 3). *DPB1*0901* was in strong LD with *DPA1*0201* and rs987870 C allele (D prime = 0.93). Because more than 90% of pediatric asthma patients were allergic to house dust mites, it is possible that the association was due to IgE reactivity (sensitization) against mites. We performed an association study for mite sensitization using independent adult subjects without allergic respiratory diseases such as asthma and perennial allergic rhinitis (367 subjects with house dust mite-specific IgE and 1633 subjects without mite-specific IgE). Subjects with house dust mite-specific IgE were non-allergic in terms of symptoms but possessed mite-specific IgE. Subjects without mite-specific IgE did not exhibit allergic symptoms. We did not find an association between rs987870 and mite sensitization ($P = 0.54$, OR = 1.07, Table S3).

Discussion

Our GWAS in Asian populations found HLA-DP as susceptibility gene for pediatric asthma. Majority of pediatric asthmas are atopic (i.e., familial tendency to produce IgE antibodies against common environmental allergens) and possess specific IgE against the house dust mite. Mite sensitization is more prevalent in Asia than in Europe and is observed in 39% of the general adult population in Japan [10]. High prevalence of mite sensitization in asthmatic children has also been reported in Taiwan, where 94.2% of children with asthma are sensitized against *Dermatophagoides pteronyssinus* [11]. However, only a small subset of subjects with house dust allergy develop asthma [12].

We performed an independent association study for mite sensitization in adult subjects without allergic respiratory diseases and did not find an association between rs987870 and mite sensitization without symptoms. If the relative risk for mite sensitization in the individuals carrying a putative risk allele was 1.4 and the allele frequency was 0.15 compared to that in individuals without the allele, the statistical power of the sample size for mite sensitization study was 0.92 at an alpha level of 0.05. These results suggested that *DPA1*0201* and *DPB1*0901* may be associated with asthma rather than IgE production against house dust mite.

The association signal was stretched in the region of *HLA-DPB2*, collagen, type XI, alpha 2 (*COL11A2*), and Retinoid X receptor beta (*RXRB*) (Figure 4). Because of LD in this region, it is difficult to specifically identify causative variants. *HLA-DPB2* is a pseudogene. *COL11A2* encodes a component of type XI collagen called the pro-alpha2(XI) chain. Mutations in *COL11A2* have been associated with non-syndromic deafness, otospondylomegaepiphyseal dysplasia, Weissenbacher-Zweymüller syndrome, and Stickler syndrome (OMIM ID *120290). RXRB belongs to the RXR family and is involved in mediating the effects of retinoic acid. RXRB forms a heterodimer with the retinoic acid receptor and thus preferentially increases its DNA binding and transcriptional activity at promoters containing retinoic acid [13]. All SNPs showing strong association with asthma ($P < 1 \times 10^{-10}$) were located in introns or intergenic regions. LD of these associated SNPs with rs987870 was not strong; therefore, it is likely that the functional effect is due to *DPA1*0201* and *DPB1*0901*.

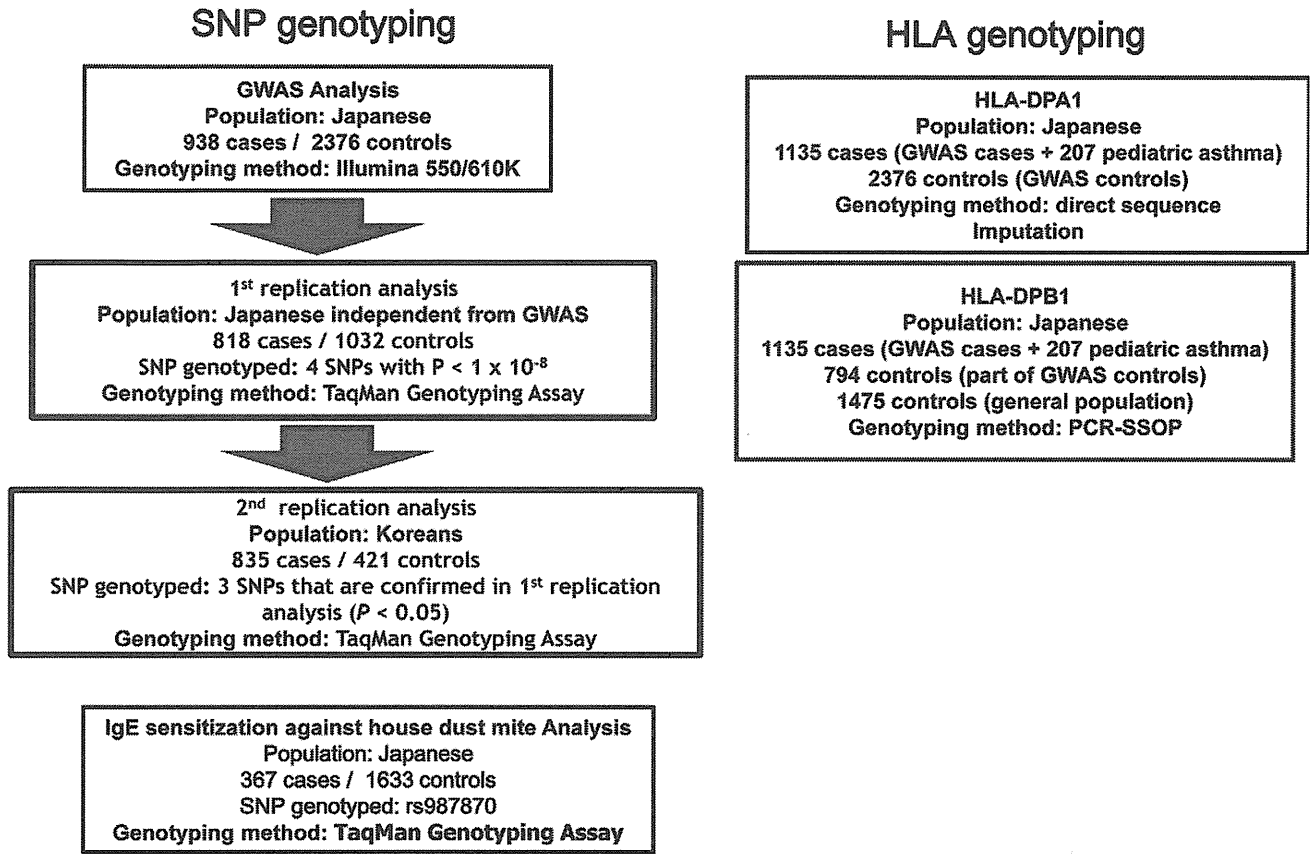

Figure 1. Flow chart of the present study.
doi:10.1371/journal.pgen.1002170.g001

In HLA-DP, Caraballo *et al.* reported that *DPB1*0401* is significantly decreased in patients with allergic asthma in Mulatto population (an admixture population of European and African ancestries) [14]. Apart from the study of Caraballo *et al.*, the association between *HLA-DP* alleles and asthma was restricted to occupational [15] or aspirin-induced asthma [16]. Howell *et al.* reported associations between HLA-DR genotype and asthma and between *HLA-DPA1*0201* and IgE specific to grass pollen mix and the pollen allergen Phl p 5 [17]. Grass pollen allergy is not a major cause of asthma in Japan [18]; therefore, the *HLA-DPA1*0201* association in the present study was less likely to be due to sensitization to grass pollen.

*DPA1*0201* has also been reported to be positively associated with lower levels of rubella-induced antibodies [19], cytokine immune responses against measles vaccine [20], and ulcerative colitis [21], and negatively associated with type 1 diabetes [22].

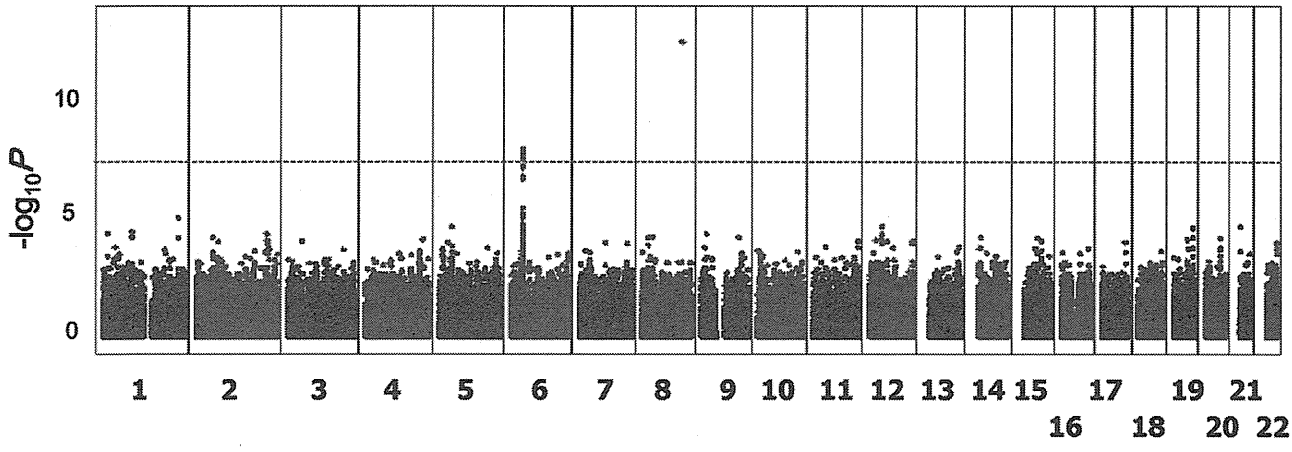

Figure 2. *P* values of GWAS. The Manhattan plot shows the Cochran–Armitage trend test *P* values for 938 cases of asthma and 2,376 controls; 450,326 autosomal SNPs were considered in the study. The dashed line indicates the genome-wide significance level ($P<5\times10-^{8}$).
doi:10.1371/journal.pgen.1002170.g002

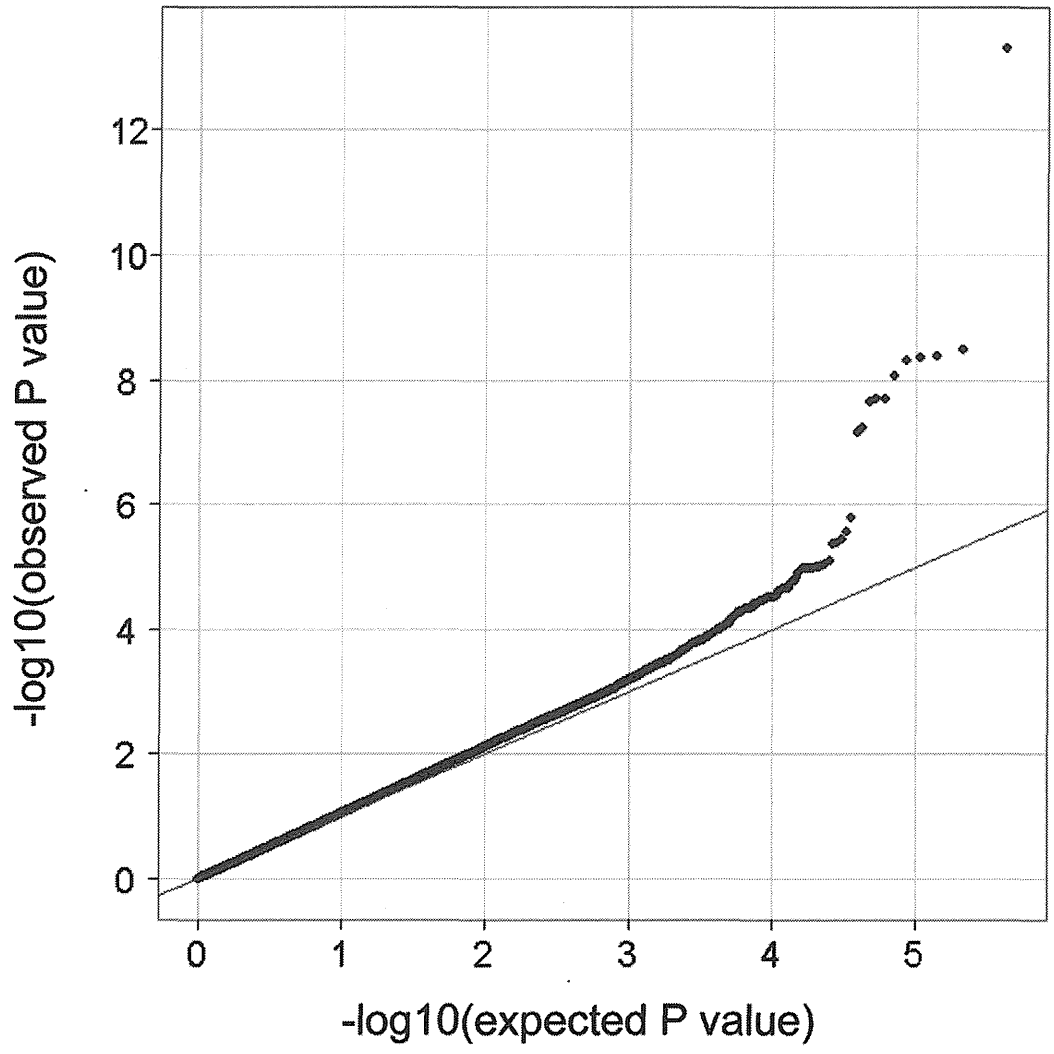

Figure 3. Quantile–quantile (Q–Q) plot of GWAS for pediatric asthma. The results of the Cochrane–Armitage trend *P* are plotted as dots and the line y = x is in red. The horizontal and vertical lines represent expected *P* values under null distribution and observed *P* values, respectively.
doi:10.1371/journal.pgen.1002170.g003

*DPB1*0901* was shown to be associated with systemic sclerosis [23], non-permissive mismatches for hematologic stem cell transplantation [24], ulcerative colitis [21], and Takayasu's arteritis [25]. *HLA-DP* molecules present short peptides of largely exogenous origin to CD4-positive helper T cells and other T cells, leading to subsequent immunological responses. T cells recognize complex formation between a specific HLA type and a particular antigen-derived epitope. Therefore, HLA molecules capable of binding a particular epitope can restrict T cell induced-immune responses, leading to association between particular HLA types and immune-related diseases. Type 1 diabetes is a Th-1 type immune disease. Varney *et al.* studied 1,771 type 1 diabetes multiplex families, analyzing them by the affected family-based control method [26], and found that *DPA1*0201* has a protective effect on the development of type 1 diabetes (adjusted $P = 5 \times 10^{-4}$, OR 0.7) [22]. Epidemiologic studies have associated type 1 diabetes with lower prevalence of asthma and other allergic diseases [26,27]. Also, the previous GWAS of rheumatoid arthritis, other Th-1 type immune disease, has shown that rs987870 C allele confers protection against rheumatoid arthritis [28]. These findings suggest that *HLA-DPA1*0201* could determine Th1/Th2 dominance and could partially explain the inverse relationship between asthma and Th-1 type immune diseases.

Previous GWAS involving European, Mexican, and African populations showed association of asthma with SNPs located in several newly discovered genes. Our GWAS dataset supported an association between identical SNPs reported in *ORMDL3/GSDMB/GSDMA*, *IL5/RAD50/IL13*, *HLA-DR/DQ*, and *SMAD3* and pediatric asthma ($P<0.05$, Table S4). Two asthma GWA studies revealed an association of HLA-DQ with pediatric/adult asthma in Caucasians [7,8]. HLA-DQ, like HLA-DP, is an αβ heterodimer of the MHC Class II type. Like HLA-DP, HLA-DQ recognizes and presents foreign antigens, but is also involved in recognizing common self-antigens and presenting those antigens to the immune system.

We failed to replicate the top SNPs of *PDE4D*, *TLE4*, *DENND1B*, *IL18R1*, and *IL2RB* that were reported in the original articles, but several SNPs in the regions surrounding *PDE4D* and *IL2RB* showed significant association when we set the significance level at $P = 0.05$ (Table S4). The different LD patterns/allele frequencies observed in *PDE4D* and *IL2RB* in Asians and Caucasians may explain the different SNP associations observed

Table 1. Results of GWAS and replication studies for 4 SNPs.

SNP	Nearest Gene	Allele[a]	Samples	MAF (asthma)	MAF (control)	OR (95%CI)[b]	P^c	P^e
rs3019885	SLC30A8	T/G	GWAS	0.41	0.31	1.55(1.39–1.73)	1.3×10^{-14}	
			First replication (Japanese)	0.34	0.30	1.21(1.05–1.39)	8.7×10^{-3}	
			Second replication (Koreans)	0.27	0.26	1.075(0.88–1.31)	4.7×10^{-1}	
			Meta analysis (HM)[d]			1.34(1.24–1.45)	5.0×10^{-13}	0.0011
rs987870	HLA-DPB1	T/C	GWAS	0.19	0.14	1.51(1.31–1.74)	7.5×10^{-9}	
			First replication (Japanese)	0.17	0.14	1.26(1.05–1.50)	1.2×10^{-2}	
			Second replication (Koreans)	0.12	0.10	1.34(1.01–1.76)	4.1×10^{-2}	
			Meta analysis (HM)[d]			1.40(1.26–1.55)	2.3×10^{-10}	0.33
rs2281389	HLA-DPB1	T/C	GWAS	0.23	0.17	1.47(1.29–1.68)	8.5×10^{-9}	
			First replication (Japanese)	0.20	0.17	1.20(1.02–1.42)	2.9×10^{-2}	
			Second replication (Koreans)	0.08	0.08	1.085(0.80–1.48)	6.1×10^{-1}	
			Meta analysis (HM)[d]			1.33(1.20–1.47)	1.4×10^{-8}	0.076

[a]The former allele represents the major allele.
[b]Odds ratio and 95% confidence interval (CI) of minor allele.
[c]*P* values of allelic model.
[d]Meta-analysis using Mantel-Haenszel approach.
[e]*P* values for heterogeneity test.
doi:10.1371/journal.pgen.1002170.t001

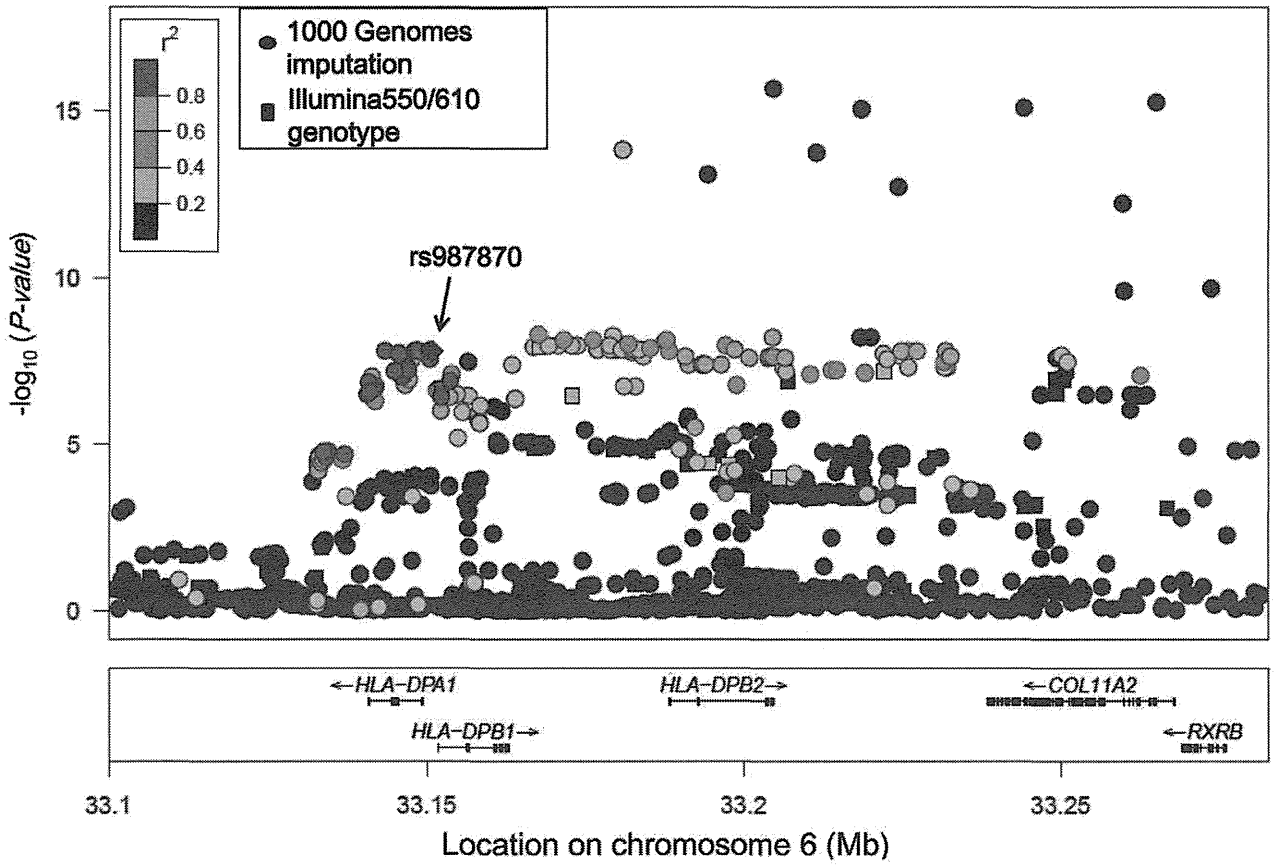

Figure 4. Association findings of genotyped (squares) and imputed (circles) SNPs in the *HLA-DP* region. SNP rs987870, which consistently showed an association with pediatric asthma in 3 independent populations, is located in the LD block between *HLA-DPA1* and *HLA-DPB1*. The color intensity of each symbol reflects the extent of LD with rs987870: from red ($r^2>0.8$) to blue ($r^2<0.2$). The physical positions are based on NCBI build 36 of the human genome.
doi:10.1371/journal.pgen.1002170.g004

Table 2. HLA-DPA1-rs987870 Haplotype analysis of pediatric asthma.

DPA1	rs987870	asthma	control	Odds ratio (95%CI)	*P* values
*DPA1*0103*	T	858(38%)	1866(39%)	0.98 (0.85–1.05)	0.29
*DPA1*0201*	C	439 (19%)	650 (14%)	1.52 (1.33–1.74)	5.5×10^{-10}
*DPA1*0202*	T	957(42%)	2223(47%)	0.83 (0.75–0.92)	0.00046
*DPA1*0401*	T	3 (0.1%)	5 (0.1%)	1.26 (0.30–5.28)	0.75

doi:10.1371/journal.pgen.1002170.t002

in different ethnic populations. rs1342326 in *IL33* was not polymorphic in the Asian population.

There were several limitations of the present GWAS. The controls for the GWAS and 1st replication samples were from adult populations. Information regarding history of asthma in early childhood or other asthma-related information (i.e., status of allergic sensitization and lung function) was not collected for these controls. Therefore, we cannot exclude the possibility that our control samples may include subjects who outgrew asthma. The prevalence of pediatric asthma in Japan is around 5%; therefore, our GWAS samples have reduced power compared with that of selected controls. In the 1st replication Japanese controls, subjects with present and past history of allergic diseases were excluded, and Korean controls in the 2nd replication were non-allergic pediatric controls (Table S5).

The genomic control value in the present study was 1.053, indicating minor population stratification. The Japanese population comprises 2 clusters (Hondo and Ryukyu; Hondo is the mainland of Japan and Ryukyu is the name of the island south of Japan). We performed principal component analysis using EIGENSTRAT software [29] to identify subjects belonging to Ryukyu. Because 2nd or 3rd generation Chinese live in Japan, and the genetic population structure in Chinese differs from that in Japanese, we also performed principal component analysis to exclude Chinese subjects. Although hidden population stratification may exist, its influence on the final results is not expected to be significant.

rs3019885 is located in intron 2 of solute carrier family 30 (SLC30A8), and showed strong association in the GWAS population. The association was replicated in the independent Japanese samples, but not in the Korean population. SLC30A8 is a zinc efflux transporter expressed at high levels only in the pancreas; the GWAS revealed that variants of *SLC30A8* are associated with type 2 diabetes [30]. Japanese and Koreans are genetically close but we cannot exclude the possibility that the association of rs3019885 with pediatric asthma is population specific.

In conclusion, we performed the first GWAS in Asian population for pediatric asthma and found that *DPA*0201/DPB1*0901* is strongly associated with pediatric asthma. The association with the HLA-DP locus emphasizes the importance of the HLA-class II molecules on the biological pathways involved in the etiology of pediatric asthma, and suggests that HLA-DP can be a therapeutic target for asthma.

Materials and Methods

Ethical statement

The study was approved by the institutional review board and the ethics committee of each institution. Written informed consent was obtained from each participant in accordance with institutional requirements and the Declaration of Helsinki Principles.

Subject participants

Characteristics of pediatric asthma cases and controls are summarized in Table S5.

GWAS population. All subjects with asthma were child or child-onset (<15 years old) asthmatics in Japan. Patients were recruited from 3 pediatric hospitals and 1 pediatric clinic, and the diagnosis of the asthma in all patients was confirmed by specialists in pediatric allergology on the basis of the criteria of the National Institutes of Health, USA, with minor modifications.

The control cases for the GWAS were healthy Japanese adult subjects from Osaka (n = 964), Tokyo (n = 660), and Ibaraki

Table 3. HLA-DPB1 allele frequency in pediatric asthma and controls.

Allele	Asthma	Control 1	Control 2	Asthma vs Control 1		Asthma vs Control 2		Asthma vs Control 1+2	
	n = 1135	n = 794	n = 1475	*P*	OR (95%CI)	*P*	OR (95%CI)	*P*	OR (95%CI)
DPB1*05:01	34.4%	36.5%	38.0%	0.18	0.91(0.80–1.04)	0.007	0.85(0.76–0.96)	0.013	0.87(0.79–0.97)
DPB1*02:01	22.4%	24.2%	24.3%	0.19	0.90(0.78–1.05)	0.11	0.89(0.79–1.02)	0.09	0.90(0.80–1.02)
DPB1*09:01	14.5%	10.1%	10.3%	5.5×10^{-5}	1.51(1.23–1.84)	3.4×10^{-6}	1.48(1.25–1.75)	2.0×10^{-7}	1.49(1.28–1.74)
DPB1*04:02	10.0%	9.2%	9.6%	0.38	1.10(0.89–1.37)	0.57	1.05(0.88–1.27)	0.43	1.07(0.90–1.27)
DPB1*04:01	4.8%	7.1%	5.0%	0.0019	0.65(0.50–0.86)	0.64	0.94(0.73–1.21)	0.08	0.82(0.65–1.03)
DPB1*03:01	4.9%	4.7%	4.0%	0.76	1.05(0.78–1.41)	0.11	1.24(0.95–1.62)	0.21	1.17(0.92–1.48)
DPB1*02:02	3.7%	3.2%	3.4%	0.46	1.14(0.80–1.63)	0.61	1.08(0.80–1.45)	0.49	1.10(0.84–1.45)
DPB1*13:01	1.6%	1.5%	2.1%	0.85	1.05(0.62–1.77)	0.18	0.75(0.50–1.14)	0.38	0.84(0.57–1.24)
DPB1*14:01	1.8%	1.7%	1.4%	0.88	1.04(0.63–1.70)	0.258	1.28(0.83–2.01)	0.39	1.19(0.80–1.76)

doi:10.1371/journal.pgen.1002170.t003

(n = 778) who had no current history of asthma [31]. In the GWAS, we genotyped 978 cases with pediatric asthma and 2402 controls using Illumina HumanHap550v3/610-Quad Genotyping BeadChip (Illumina, San Diego, USA). Subjects from Osaka and Ibaraki were randomly selected from residents of Suita city and Tone town, respectively. Subjects from Tokyo were hospital workers from Keio University Hospital, Tokyo. We excluded samples considered duplicated, related (first- or second-degree relatives), or belonging to Han Chinese or Ryukyu. In total, 938 cases and 2376 controls were considered for further analysis.

First replication population (Japanese). We recruited 818 subjects with childhood atopic asthma from the Osaka Prefectural Medical Center for Respiratory and Allergic Diseases, Dokkyo University School of Medicine, National Research Institute for Child Health & Development, National Sagamihara Hospital, and Chiba University Hospital. All subjects with bronchial asthma were diagnosed according to the criteria of the National Institutes of Health (National Heart, Lung, and Blood Institute, National Institutes of Health, 1991) by physicians who were asthma specialists [32,33]. After the exclusion of individuals who had been diagnosed with asthma, atopic dermatitis, or nasal allergies by physicians' interviews, 825 healthy individuals were recruited from the Midousuji Rotary Club [32,33]. Two hundred and seven control subjects who never had the symptoms of allergic rhinitis/asthma and did not show any sensitization to 7 common aeroallergens were recruited from Fukui [34].

Second replication population (Korean). Patients with pediatric asthma were enrolled at Asan Medical Center, University of Ulsan College of Medicine, Seoul, Korea. The control subjects were age-matched children with no history of asthma or other allergic diseases, negative skin prick test, and normal total IgE values (<100 IU/mL) recruited from the same district (Seoul). Total of 835 cases and 421 controls participated in this study. The details of the patients and controls were described in a previous study [35].

Subjects for IgE sensitization against house dust mite. General populations for mite sensitivity study were recruited from Fukui [10] and Tsukuba in Japan. Total and specific IgE levels (produced in response to Japanese cedar, *Dermatophagoides*, *Dactylis glomerata*, *Ambrosia artemisiifolia*, *Candida albicans*, and *Aspergillus*) were measured using the CAP-RAST method (for Fukui samples; Pharmacia Diagnostics AB, Uppsala, Sweden) or MAST-26 (for Tsukuba samples; Hitachi Chemical Co. Ltd., Tokyo, Japan). Positive sensitization against house dust mite was defined as specific IgE levels against the house dust mite (*Dermatophagoides farinae* or *Dermatophagoides pteronyssinus*) greater than or equal to 0.70 IU/ml (class 2) or lumicount greater than 2.76 (class 2). Subjects with asthma (current or past) or perennial allergic rhinitis were excluded from the analysis. Sensitized subjects (Mite-positive) were non-allergic in terms of symptoms but possessed mite-specific IgE. Non-sensitized subjects (Mite-negative) did not show any allergic symptoms and did not have mite-specific IgE.

Subjects for *HLA-DPA1* typing. Cases with asthma included 938 subjects used in GWAS analysis and 207 Japanese subjects with child- or child-onset (<15 years) asthmatics recruited in Tsukuba. The diagnosis of asthma in all patients was confirmed by specialists in pediatric allergology on the basis of the criteria of the National Institutes of Health, USA, with minor modifications. The control subjects were 2378 subjects that were used in GWAS analysis. Because most of the DNA from the GWAS controls was not available for genotyping, and we found that imputation of the *HLA-DPA1* allele using GWAS results was highly accurate (error rate, 0.003), we decided to genotype the *HLA-DPA1* allele by direct sequencing and imputation. Among the subjects for *HLA-DPA1* genotyping (1135 cases and 2376 controls), genotyping of 383 subjects was performed by direct sequencing and genotyping of the remaining 3128 samples was performed by imputation.

Subjects for *HLA-DPB1* typing. Cases with asthma included 938 subjects used in GWAS analysis and 207 Japanese subjects with child- or child-onset (<15 years) asthmatics; the same as those used in *HLA-DPA1* typing. The control 1 subjects for *HLA-DPB1* typing were 794 healthy adult subjects from Tokyo and 399 subjects were the same as those in GWAS. The control 2 subjects (n = 1475) were general datasets from Japanese population samples publically available at http://www.hla.or.jp/hapro/top.html. Because most of the DNA from the GWAS controls was not available for genotyping, and the imputation of the DPB1 allele using the GWAS results was not possible, we used 794 healthy adult subjects from Tokyo and 399 subjects from the GWAS for *DPB1* genotyping (Control 1). The control 2 subjects (n = 1475) were general datasets from Japanese population samples publically available at http://www.hla.or.jp/hapro/top.html. The status of asthma or other allergic diseases for these samples is not available.

Genotyping

Genotyping for GWAS was performed using the Illumina HumanHap550v3/610-Quad Genotyping BeadChip (Illumina), as per manufacturer's instruction.

In replication analyses, genotyping of each individual was performed with the TaqMan genotyping system (Applied Biosystems) on an ABI PRISM 7900HT Sequence Detection System (Applied Biosystems). PCR was performed on a 384-well format, and automatic allele calling was performed using ABI PRISM 7900HT data collection and analysis software, version 2.2.2 (Applied Biosystems).

HLA-DPB1 genotyping of 1135 cases, 794 controls (control 1) and 1475 controls (control 2) were performed with the WAKFlow HLA typing kit (Wakunaga, Hiroshima, Japan), as per manufacturer's instruction. First, the target DNA was amplified by polymerase chain reaction (PCR) with biotinylated primers specifically designed for each HLA-DPB1 locus. Then, the PCR product was denatured and hybridized to complementary oligonucleotide probes immobilized on fluorescent-coded microsphere beads. Concurrently, the biotinylated PCR product was labeled with phycoerythrin-conjugated streptavidin and immediately examined with the Luminex 100 system (Luminex, Austin, TX). Genotype determination and data analysis were performed with the WAKFlow typing software (Wakunaga).

HLA-DPA1 genotyping was performed with direct sequencing of exon 2 with forward primer 5′-TCAGGATGCCCAGACTTTCAA-3′ and reverse primer 5′-CAGGGGGCACTTAGGCTTCC-3′, and with the sequencing primer 5′-TCAGGATGCCCAGACTTTCAA-3′ using the BigDye Terminator v.1.1 Cycle Sequencing Kit (Applied Biosystems) on an ABI PRISM 3130 Genetic Analyzer (Applied Biosystems).

Statistical analysis

In the GWAS, we examined the potential genetic relatedness on the basis of pairwise identity by state for all of the successfully genotyped samples using the EIGENSTRAT software [29]. In the GWAS, we genotyped 978 cases with pediatric asthma and 2402 controls using Illumina HumanHap550v3/610-Quad Genotyping BeadChip (Illumina, San Diego, USA). Samples of duplicated (identical individual or monozygotic twin), first-, second-, and third-degree pairs were detected, and the individual with a lower call rate was excluded from further analysis. PCA was performed, and the results were combined with those obtained for our in-

house Ryukyu and Han Chinese reference samples. Yamaguchi-Kabata *et al.* characterized the Japanese population structure using the genotypes for 140,387 SNPs in 7003 Japanese individuals, along with 60 European, 60 African, and 90 East-Asian individuals, in the HapMap project and found that the Japanese population is composed of 2 clusters (Hondo and Ryukyu) [36]. Hondo is the biggest island of Japan, and the island of Ryukyu is located in southern Japan. Also, we have 2nd or 3rd generation Chinese living in Japan, and Chinese present a different genetic population structure from Japanese. Therefore, we excluded samples belonging to Han Chinese or Ryukyu, and 938 cases and 2376 controls were considered for further analysis.

Cluster plots of SNPs were checked by visual inspection and SNPs with ambiguous calls were excluded. We excluded SNPs with a low genotyping rate (<90%), minor allele frequency less than 0.01 in either pediatric asthma cases or controls, or with Hardy-Weinberg equilibrium P value$<10^{-4}$ in controls. Finally, 450,326 SNPs were used for the GWAS. Details regarding the exact number of remaining SNPs after applying each quality control criterion are available in Table S1.

The genomic control inflation factor (λ_{GC}), defined as the median association test statistic across all SNPs divided by its expected value, was calculated by the method proposed by Devlin *et al.* [37]. GWAS and replication analyses were performed using the Cochran–Armitage trend test and χ^2 test. The meta-analysis was performed with the Mantel–Haenszel approach as a fixed-effects model [38]. All statistical findings were reported without correction. The results of GWAS were plotted with GWAS GUI v0.0.2 [39]. HLA-DP region was plotted with LocusZoom [40]. The power calculation was performed with Genetic Power Calculator [41]. Quantile-quantile (Q-Q) plot was plotted with ggplot2 package [42] in R version 2.10.0 (http://www.r-project.org/).

Imputation of genotypes in the DP region was performed with MACH version 1.0 [9] with 1000 Genome Project data (1000G 2010-6 release, http://www.sph.umich.edu/csg/yli/mach/download/1000G-2010-06.html).

HLA-DPA1 allele imputation

The HLA-DP region was in strong linkage disequilibrium and some DPB1 alleles were known to be linked with particular DPA1 alleles. First, we imputed HLA-DPA1 alleles by using the actual genotype data of samples obtained from Illumina HumanHap550v3/610-Quad (Illumina) and 1000 Genome Project data of Asian origin (JPT+CHB) (http://www.sph.umich.edu/csg/abecasis/MaCH/download/1000G-2010-06.html). The accuracy of the imputated data was confirmed by direct sequencing. The error rate of imputation was 1/352 (0.003).

Supporting Information

Table S1 Number of remaining SNPs after applying each quality control criterion.
(XLS)

Table S2 SNPs that are strong linkage disequilibrium ($r^2>0.9$) with rs987870.
(XLS)

Table S3 Association analysis for mite IgE sensitization.
(XLS)

Table S4 Genotyping data of the Japanese pediatric asthma GWAS.
(XLS)

Table S5 Characteristics of cases and controls.
(XLS)

Acknowledgments

We would like to thank the study participants for their participation of this study. We also thank for Dr. Toshio Abe, Dr. Hironobu Fukuda, and Dr. Mitsuhiro Nishida at Dokkyo Medical University, for collecting samples. We also thank Ms. Sumiko Ohnami (Division of Genetics, National Cancer Center Research Institute, Tokyo, Japan) for excellent technical support for genotyping and Mr. Shuhei Fukuda (Department of Allergy and Immunology, National Research Institute for Child Health and Development, Tokyo, Japan) for excellent technical support. We thank Naoharu Iwai (Department of Genomic Medicine, National Cerebral and Cardiovascular Center, Osaka, Japan) and Hitonobu Tomoike (Department of Preventive Cardiology, National Cerebral and Cardiovascular Center, Osaka, Japan) for providing genotype and phenotype information of Suita study. We thank Dr. Hirohiko Totsuka (Genetics Division, National Cancer Center Research Institute, and Bioinfomatics Group, Research and Development Center, Hitachi Government and Public Corporation System Engineering Ltd., Tokyo, Japan) for statistical analysis. We thank Dr. Saji at HLA laboratory for his technical support of HLA genotyping.

Author Contributions

Conceived and designed the experiments: E Noguchi, K Matsumoto. Performed the experiments: S Yoshihara, S-J Hong, Y Goto, T Asada, S Fujieda, N Hizawa, Y Nakamura, M Tamari, T Arinami, T Yoshida, Y Suzuki, H Sakamoto. Analyzed the data: H Saito, T Hirota, K Ochiai, M Sakashita. Contributed reagents/materials/analysis tools: Y Imoto, F Kurosaka, A Akasawa, N Shimojo, Y Kohno, N Kanno, Y Yamada, M-J Kang, J-W Kwon, F Yamashita, K Inoue, H Hirose, I Saito, T Sakamoto, H Masuko, I Nomura. Wrote the paper: E Noguchi, K Matsumoto.

References

1. Kusunoki T, Morimoto T, Nishikomori R, Yasumi T, Heike T, et al. (2009) Changing prevalence and severity of childhood allergic diseases in kyoto, Japan, from 1996 to 2006. Allergol Int 58: 543–548.
2. Pawankar R, Bunnag C, Chen Y, Fukuda T, Kim YY, et al. (2009) Allergic rhinitis and its impact on asthma update (ARIA 2008)–western and Asian-Pacific perspective. Asian Pac J Allergy Immunol 27: 237–243.
3. Moffatt MF, Kabesch M, Liang L, Dixon AL, Strachan D, et al. (2007) Genetic variants regulating ORMDL3 expression contribute to the risk of childhood asthma. Nature 448: 470–473.
4. Himes BE, Hunninghake GM, Baurley JW, Rafaels NM, Sleiman P, et al. (2009) Genome-wide association analysis identifies PDE4D as an asthma-susceptibility gene. Am J Hum Genet 84: 581–593.
5. Hancock DB, Romieu I, Shi M, Sienra-Monge JJ, Wu H, et al. (2009) Genome-wide association study implicates chromosome 9q21.31 as a susceptibility locus for asthma in mexican children. PLoS Genet 5: e1000623. doi:10.1371/journal.pgen.1000623.
6. Sleiman PM, Flory J, Imielinski M, Bradfield JP, Annaiah K, et al. (2010) Variants of DENND1B associated with asthma in children. N Engl J Med 362: 36–44.
7. Li X, Howard TD, Zheng SL, Haselkorn T, Peters SP, et al. (2010) Genome-wide association study of asthma identifies RAD50-IL13 and HLA-DR/DQ regions. J Allergy Clin Immunol 125: 328–335 e311.
8. Moffatt MF, Gut IG, Demenais F, Strachan DP, Bouzigon E, et al. (2010) A large-scale, consortium-based genomewide association study of asthma. N Engl J Med 363: 1211–1221.
9. Li Y, Willer C, Sanna S, Abecasis G (2009) Genotype imputation. Annu Rev Genomics Hum Genet 10: 387–406.
10. Imoto Y, Enomoto H, Fujieda S, Okamoto M, Sakashita M, et al. (2010) S2554X mutation in the filaggrin gene is associated with allergen sensitization in the Japanese population. J Allergy Clin Immunol 125: 498–500 e492.
11. Huang HW, Lue KH, Wong RH, Sun HL, Sheu JN, et al. (2006) Distribution of allergens in children with different atopic disorders in central Taiwan. Acta Paediatr Taiwan 47: 127–134.

12. Shibasaki M, Noguchi E, Takeda K, Takita H (1997) Distribution of IgE and IgG antibody levels against house dust mites in schoolchildren, and their relation with asthma. J Asthma 34: 235–242.
13. Yu VC, Delsert C, Andersen B, Holloway JM, Devary OV, et al. (1991) RXR beta: a coregulator that enhances binding of retinoic acid, thyroid hormone, and vitamin D receptors to their cognate response elements. Cell 67: 1251–1266.
14. Caraballo L, Marrugo J, Jimenez S, Angelini G, Ferrara GB (1991) Frequency of DPB1*0401 is significantly decreased in patients with allergic asthma in a mulatto population. Hum Immunol 32: 157–161.
15. Choi JH, Lee KW, Kim CW, Park CS, Lee HY, et al. (2009) The HLA DRB1*1501-DQB1*0602-DPB1*0501 haplotype is a risk factor for toluene diisocyanate-induced occupational asthma. Int Arch Allergy Immunol 150: 156–163.
16. Choi JH, Lee KW, Oh HB, Lee KJ, Suh YJ, et al. (2004) HLA association in aspirin-intolerant asthma: DPB1*0301 as a strong marker in a Korean population. J Allergy Clin Immunol 113: 562–564.
17. Howell WM, Standring P, Warner JA, Warner JO (1999) HLA class II genotype, HLA-DR B cell surface expression and allergen specific IgE production in atopic and non-atopic members of asthmatic family pedigrees. Clin Exp Allergy 29 Suppl 4: 35–38.
18. Shibasaki M, Hori T, Shimizu T, Isoyama S, Takeda K, et al. (1990) Relationship between asthma and seasonal allergic rhinitis in schoolchildren. Ann Allergy 65: 489–495.
19. Ovsyannikova IG, Jacobson RM, Vierkant RA, O'Byrne MM, Poland GA (2009) Replication of rubella vaccine population genetic studies: validation of HLA genotype and humoral response associations. Vaccine 27: 6926–6931.
20. Ovsyannikova IG, Ryan JE, Jacobson RM, Vierkant RA, Pankratz VS, et al. (2006) Human leukocyte antigen and interleukin 2, 10 and 12p40 cytokine responses to measles: is there evidence of the HLA effect? Cytokine 36: 173–179.
21. Yoshitake S, Kimura A, Okada M, Yao T, Sasazuki T (1999) HLA class II alleles in Japanese patients with inflammatory bowel disease. Tissue Antigens 53: 350–358.
22. Varney MD, Valdes AM, Carlson JA, Noble JA, Tait BD, et al. (2010) HLA DPA1, DPB1 alleles and haplotypes contribute to the risk associated with type 1 diabetes: analysis of the type 1 diabetes genetics consortium families. Diabetes 59: 2055–2062.
23. Zhou X, Lee JE, Arnett FC, Xiong M, Park MY, et al. (2009) HLA-DPB1 and DPB2 are genetic loci for systemic sclerosis: a genome-wide association study in Koreans with replication in North Americans. Arthritis Rheum 60: 3807–3814.
24. Zino E, Frumento G, Marktel S, Sormani MP, Ficara F, et al. (2004) A T-cell epitope encoded by a subset of HLA-DPB1 alleles determines nonpermissive mismatches for hematologic stem cell transplantation. Blood 103: 1417–1424.
25. Kimura A, Kitamura H, Date Y, Numano F (1996) Comprehensive analysis of HLA genes in Takayasu arteritis in Japan. Int J Cardiol 54 Suppl: S61–69.
26. Thomsen SF, Duffy DL, Kyvik KO, Skytthe A, Backer V (2010) Relationship between type 1 diabetes and atopic diseases in a twin population. Allergy.
27. Tzeng ST, Hsu SG, Fu LS, Chi CS (2007) Prevalence of atopy in children with type 1 diabetes mellitus in central Taiwan. J Microbiol Immunol Infect 40: 74–78.
28. Plenge RM, Seielstad M, Padyukov L, Lee AT, Remmers EF, et al. (2007) TRAF1-C5 as a risk locus for rheumatoid arthritis–a genomewide study. N Engl J Med 357: 1199–1209.
29. Price AL, Patterson NJ, Plenge RM, Weinblatt ME, Shadick NA, et al. (2006) Principal components analysis corrects for stratification in genome-wide association studies. Nat Genet 38: 904–909.
30. Sladek R, Rocheleau G, Rung J, Dina C, Shen L, et al. (2007) A genome-wide association study identifies novel risk loci for type 2 diabetes. Nature 445: 881–885.
31. Hiura Y, Tabara Y, Kokubo Y, Okamura T, Miki T, et al. (2010) A genome-wide association study of hypertension-related phenotypes in a Japanese population. Circ J 74: 2353–2359.
32. Harada M, Nakashima K, Hirota T, Shimizu M, Doi S, et al. (2007) Functional polymorphism in the suppressor of cytokine signaling 1 gene associated with adult asthma. Am J Respir Cell Mol Biol 36: 491–496.
33. Hirota T, Suzuki Y, Hasegawa K, Obara K, Matsuda A, et al. (2005) Functional haplotypes of IL-12B are associated with childhood atopic asthma. J Allergy Clin Immunol 116: 789–795.
34. Sakashita M, Yoshimoto T, Hirota T, Harada M, Okubo K, et al. (2008) Association of serum interleukin-33 level and the interleukin-33 genetic variant with Japanese cedar pollinosis. Clin Exp Allergy 38: 1875–1881.
35. Kim HB, Kang MJ, Lee SY, Jin HS, Kim JH, et al. (2008) Combined effect of tumour necrosis factor-alpha and interleukin-13 polymorphisms on bronchial hyperresponsiveness in Korean children with asthma. Clin Exp Allergy 38: 774–780.
36. Yamaguchi-Kabata Y, Nakazono K, Takahashi A, Saito S, Hosono N, et al. (2008) Japanese population structure, based on SNP genotypes from 7003 individuals compared to other ethnic groups: effects on population-based association studies. Am J Hum Genet 83: 445–456.
37. Devlin B, Roeder K (1999) Genomic control for association studies. Biometrics 55: 997–1004.
38. Petitti D (2000) Meta-Analysis, Decision Analysis, and Cost-Effective Analysis Second Edition Second Edition Oxford university pres.
39. Chen W, Liang L, Abecasis GR (2009) GWAS GUI: graphical browser for the results of whole-genome association studies with high-dimensional phenotypes. Bioinformatics 25: 284–285.
40. Pruim RJ, Welch RP, Sanna S, Teslovich TM, Chines PS, et al. (2010) LocusZoom: regional visualization of genome-wide association scan results. Bioinformatics 26: 2336–2337.
41. Purcell S, Cherny SS, Sham PC (2003) Genetic Power Calculator: design of linkage and association genetic mapping studies of complex traits. Bioinformatics 19: 149–150.
42. Wickham H (2009) ggplot2: elegant graphics for data analysis Springer New York.

The American Journal of Pathology, Vol. 180, No. 1, January 2012

DOI: 10.1016/j.ajpath.2011.09.013

Growth Factors, Cytokines, and Cell Cycle Molecules

Blockade of Interleukin-6 Receptor Alleviates Disease in Mouse Model of Scleroderma

Shun Kitaba,* Hiroyuki Murota,* Mika Terao,* Hiroaki Azukizawa,* Fumitaka Terabe,† Yoshihito Shima,‡ Minoru Fujimoto,† Toshio Tanaka,‡ Tetsuji Naka,† Tadamitsu Kishimoto,§ and Ichiro Katayama*

From the Department of Dermatology, Course of Integrated Medicine and the Department of Respiratory Medicine, Allergy and Rheumatic Diseases,‡ Graduate School of Medicine, Osaka University, Osaka; the Laboratory for Immune Signal,† National Institute of Biomedical Innovation, Osaka; and the Laboratory of Immune Regulation,§ Osaka University Graduate School of Frontier Biosciences, Osaka, Japan*

Activation of fibroblasts by interleukin-6 (IL-6) is implicated in the pathogenesis of scleroderma, suggesting that the inhibition of fibroblast activation may be a promising scleroderma treatment. In this study, we used an IL-6 blocking antibody (Ab) and *Il-6* knockout (Il-6KO) mice to examine the role of IL-6 in the bleomycin (BLM)-induced mouse model of scleroderma. BLM was administered to C57BL/6 and *Il-6*KO mice to induce dermal sclerosis. BLM-treated and control phosphate-buffered saline-treated mice were treated with anti-mouse IL-6 receptor monoclonal Ab (MR16-1). Disease severity was evaluated by measuring dermal thickness and skin hardness, by counting the numbers of α-smooth muscle actin-positive cells and mast cells, and by examining the cutaneous draining lymph nodes. C57BL/6 mice with BLM induced scleroderma had elevated serum IL-6 levels and more severe dermal sclerosis than *Il-6*KO mice. Weekly administration of MR16-1, but not control Ab, prevented and improved dermal sclerosis, and also attenuated swelling of the draining lymph nodes. MR16-1 suppressed α-smooth muscle actin induction in IL-6–stimulated *Il-6*KO fibroblasts. Our results indicate that IL-6 contributes to BLM induced dermal sclerosis and that IL-6 receptor–specific monoclonal Ab may improve the symptoms of scleroderma by suppressing fibroblast activation. *(Am J Pathol 2012, 180:165–176; DOI: 10.1016/j.ajpath.2011.09.013)*

Patients with scleroderma frequently experience broad area skin sclerosis and internal organ involvement including pulmonary fibrosis, esophageal dysfunction, pulmonary arterial hypertension, renal crisis, and heart failure.[1] These symptoms dramatically affect the prognosis for scleroderma patients. Autoaggressive immunological activation and continuous activation of fibroblasts are the key components of scleroderma, yet the mechanisms underlying these are incompletely understood.

Several lines of evidence indicate that interleukin (IL)-6 contributes to the disease process in scleroderma. Serum IL-2, IL-4, IL-6, and tumor necrosis factor α levels are elevated in scleroderma.[2–6] Increased serum IL-6 levels are also observed in both scleroderma mouse models: the bleomycin (BLM)-induced scleroderma mouse and the type 1 tight-skin mouse (*Tsk1/*$^{+}$).[7,8] At the cellular level, IL-6–producing T helper type 2 clones contribute to anti-DNA topoisomerase I autoantibody, a key autoantibody in scleroderma.[9] The point of action of IL-6 in scleroderma remains controversial, with some evidence suggesting the final maturation step of B cells[10] and/or activation of fibroblasts.[11–13] Thus, although the specific function of IL-6 in the pathogenesis of scleroderma remains unclear, there is ample evidence that inhibition of IL-6–mediated signaling might be a route to better treatment for scleroderma.

In this study, we used the BLM-induced scleroderma mouse model to demonstrate the importance of IL-6 in pathogenesis of scleroderma and to evaluate the effect of anti-mouse IL-6 receptor monoclonal antibody. We have examined whether MR16-1 acts directly on dermal fibroblasts by investigating the induction of myofibroblasts *in vitro*. We also examined the tissue of scleroderma patients treated with tocilizumab, a humanized monoclonal antibody (Ab) against the IL-6 receptor used to treat rheumatoid arthritis or Castleman's disease.[14] Patients

Supported by the Program for Promotion of Fundamental Studies in Health Sciences of the National Institute of Biomedical Innovation.

Accepted for publication September 21, 2011.

Disclosure: T.K. holds a patent for tocilizumab. All other authors have no conflicts of interest to declare.

Address for reprint requests: Hiroyuki Murota, M.D., Ph.D., 2-2, Yamadaoka, Suita-Shi, Osaka, Japan 565-0871. E-mail: h-murota@derma.med.osaka-u.ac.jp.

with intractable scleroderma treated with tocilizumab were previously reported to show marked amelioration of dermal sclerosis.[15] Our results indicate that IL-6 induces dermal sclerosis via direct activation of dermal fibroblasts and that biomolecular targeting to suppress IL-6 might be a promising therapeutic approach for scleroderma.

Materials and Methods

Dermal Fibroblast Isolation and Culture

The dermis was collected and separated from the epidermis as described previously.[4,16] Briefly, newborn wild-type and *Il-6* knockout (KO) mouse pups (age 2 to 4 days) were sacrificed and rinsed in 70% ethanol. The skin was excised and treated with 4 mg/mL of dispase (Gibco, Invitrogen, Paisley, UK) for 1 hour at 37°C. The dermis was then separated from the epidermis, placed in phosphate-buffered saline (PBS) + 0.05% type-1 collagenase (Sigma-Aldrich, St. Louis, MO), and incubated at 37°C for 30 minutes with vigorous agitation to prepare single cells. After filtration, cells were resuspended in Dulbecco's modified Eagle's medium + 10% fetal bovine serum and incubated at 37°C and 5% CO_2.

The primary *Il-6*KO fibroblasts were passaged once or twice and used for subsequent experiments. Cells were confirmed to have the classical morphology (long spindle shape) of fibroblasts.

Patients and Skin Samples

This study included two scleroderma patients treated with tocilizumab and three scleroderma patients not treated with tocilizumab. Two scleroderma patients were treated with 8 mg/kg of tocilizumab monthly for 6 months with the permission of the Ethics Committee of Osaka University Hospital and after receipt of informed consent. Detailed patient information was described previously.[15] Skin samples were obtained from patients before and after treatment. Written informed consent was obtained from all patients before skin biopsy.

Immunofluorescent Staining

Wild-type (C57BL/6) and *Il-6*KO fibroblasts were cultured to semiconfluence in 350-mm culture plates. The cultures were fixed in 4% paraformaldehyde at room temperature for 10 minutes and permeabilized with 0.5% Triton in PBS for 5 minutes. The primary Abs used were mouse monoclonal anti–α-smooth muscle actin Ab (1:100, α-SMA; Dako-Cytomation, Carpinteria, CA) , After 1 hour incubation, cells were stained for 30 minutes with Alexa Fluor 488 anti-mouse IgG secondary Ab to α-SMA (Invitrogen, Carlsbad, CA) and Hoechst 33342 (Molecular Probes, Eugene, OR). Mouse IgG_{2a} (Dako-Cytomation, Carpinteria, CA) was used as a control for nonspecific staining.

Paraffin-embedded sections derived from scleroderma patients treated with 6 months of tocilizumab or 6 months of prednisolone, and redundant tissue from surgical specimens were deparaffinized and hydrated. Skin sections derived from patients were brought to a boil in 10 mmol/L sodium citrate buffer (pH 6.0) and then maintained at a subboiling temperature for 10 minutes. After blocking with 5% normal goat serum (Vector Laboratories, Burlingame, CA) in PBST, they were double-stained with mouse monoclonal anti–α-SMA Ab (Dako-Cytomation) and rabbit monoclonal phospho-p44/42 MAPK Ab (Cell Signaling, Beverly, MA). Secondary antibodies were as follows: anti-mouse Alexa Fluor 488 for α-SMA Ab and biotinylated anti-rabbit IgG (Vector Laboratories) plus DyLight594-conjugated Streptavidin (Jackson ImmunoResearch Laboratories, West Grove, PA) for phospho-p44/42 MAPK Ab. Images of immunolabeled sections were captured with a BZ-8000 microscope (Keyence, Osaka, Japan).

Table 1. Effect of MR16-1 on BLM-Induced Dermal Sclerosis in a Prevention Model

	Thickness (mm)			Hardness (Arbitrary)		
	1st (n = 4)	2nd (n = 4)	3rd (n = 4)	1st (n = 4)	2nd (n = 4)	3rd (n = 4)
PBS						
Control Ab	0.137 ± 0.016	0.10 ± 0.01	0.123 ± 0.010	7.09 ± 2.17	6.14 ± 0.72	4.86 ± 1.05
MR16-1	0.11 ± 0.01	0.111 ± 0.011	0.122 ± 0.013	8.91 ± 2.59	6.45 ± 1.49	4.92 ± 0.77
% Change						
Each experiment	81.82	106.33	98.65	125.64	104.91	101.15
Mean ± SE		95.60 ± 7.238			110.6 ± 7.614	
BLM						
Control Ab	0.33 ± 0.04*	0.36 ± 0.05*	0.30 ± 0.07*	24.14 ± 5.58*	16.61 ± 1.90*	9.93 ± 1.51*
MR16-1	0.22 ± 0.03†‡	0.29 ± 0.02‡§	0.16 ± 0.03†	15.47 ± 4.52	8.53 ± 0.80†	5.92 ± 0.49†
% Change						
Each experiment	67.09	81.29	52.22	64.08	51.33	59.59
Mean ± SE		66.89 ± 8.39			58.34 ± 3.74	

(*table continues*)

Values are mean ± SD. To quantify the impact of BLM treatment, % changes were calculated as follows: (evaluative consequences of BLM treatment/that of PBS treatment) × 100 (%).

*$P < 0.01$ PBS+Control Ab versus BLM+Control Ab.

†$P < 0.01$ BLM+Control Ab versus BLM+MR16-1.

‡$P < 0.01$ PBS+MR16-1 versus BLM+MR16-1.

§$P < 0.05$ BLM+Control Ab versus BLM+MR16-1.

HPS, high-power field.

Western Blot Analysis

Wild-type and *Il-6*KO fibroblasts were prepared as described above and cultured to semiconfluence in 100-cm^2 culture plates. Before treatment, fibroblast cultures were washed twice with PBS, and culture media were replaced with low-serum (0.1%fetal bovine serum) Dulbecco's modified Eagle's medium containing 60 IU/mL penicillin, 100 IU/mL streptomycin, and 4 mmol/L glutamine. Low-serum medium was necessary to maintain viability of primary fibroblasts overnight.

Following 12 hours incubation in low-serum medium, treatments were applied to the cultures in fresh low-serum Dulbecco's modified Eagle's medium. Semiconfluent cultures were treated with 10 ng/mL of MR16-1 or 10 μmol/L of PD98058 (Calbiochem, San Diego, CA) for 3 hours, and then 10 ng/mL of recombinant mouse IL-6 (R&D Systems, Minneapolis, MN) was added to the cultures for 24 hours. At indicated time points, culture plates were rinsed twice with ice-cold PBS, and total cell protein was collected in 500 μL of lysis buffer [50 mmol/L Tris-HCl (pH 7.6), 150 mmol/L NaCl, 1% deoxycholic acid, 0.1% sodium dodecyl sulfate, 1% Triton X-100, 1 mmol/L sodium orthovanadate, and protease inhibitor cocktail]. Western blot analysis was performed as previously described.[4] Ten micrograms of protein were fractionated on SDS-polyacrylamide gels and transferred onto PVDF membranes (Bio-Rad, Hercules, CA). Nonspecific protein binding was blocked by incubating the membranes in 5% w/v nonfat milk powder in TBST [50 mmol/L Tris-HCl (pH 7.6), 150 mmol/L NaCl, and 0.1% v/v Tween-20]. The membranes were incubated with mouse monoclonal anti–α-SMA (Dako-Cytomation) Ab at a dilution of 1:1000 overnight at 4°C or with mouse monoclonal anti–β-actin (Sigma-Aldrich) at a dilution of 1:5000 for 30 minutes at room temperature. After three 5-minute washes in TBST, membranes were incubated with horseradish peroxidase–conjugated anti-mouse Ab at a dilution of 1:10,000 for 60 minutes at room temperature. Protein bands were detected using the ECL Plus kit (GE Healthcare, Little Chalfont, UK). Western blot quantification was performed with ImageJ software (NIH, Bethesda, MD) and used to visualize fold expression differences between these treatment groups.

Mice and Induction of Skin Sclerosis

Six-week-old female mice were used in all experiments. C57BL/6 mice were purchased from Japan Clea (Osaka, Japan). Mutant C57BL/6 mice rendered null for IL-6 were described previously[17] and were purchased from the National Institute of Biomedical Innovation (Osaka, Japan). Mice were maintained in our pathogen-free animal facility. All animal care was in accordance with the institutional guidelines of Osaka University. BLM (Nippon Kayaku, Tokyo, Japan) was dissolved in PBS at a concentration of 1 mg/mL and sterilized by filtration. BLM (0.1 mg/100 μL) was injected subcutaneously into the shaved back of the mice daily for 4 weeks with a 27-gauge needle as described by Yamamoto et al.[7] Control mice received 100 μL of PBS instead.

RNA Isolation and Real-Time PCR

Sections of skin lesions and the cutaneous draining lymph nodes (LNs) were removed 1 day after the final injection. Total RNA was isolated using the SV Total RNA Isolation System (Promega, Madison, WI) and reverse transcribed into complementary DNA.

IL-6 expression was measured using the Power SYBR Green PCR Master Mix (Applied Biosystems, Foster City, CA) according to the manufacturer's protocol. Glyceraldehyde-3-phosphate dehydrogenase (GAPDH) was used to normalize the mRNA. Sequence-specific primers were: IL-6, sense 5′-ACACACTGGTTCTGAGGGAC-3′, antisense 5′-TACCACAAGGTTGGCAGGTG-3′; GAPDH,

Table 1. *Continued*

α-SMA–Positive Cells (Cells/HPS)			Mast Cells (Cells/HPS)		
1st (n = 4)	2nd (n = 4)	3rd (n = 4)	1st (n = 4)	2nd (n = 4)	3rd (n = 4)
6.00 ± 4.08 5.00 ± 1.73	3.50 ± 1.29 4.00 ± 1.41	8.75 ± 1.50 10.00 ± 4.16	12.50 ± 4.51 11.00 ± 1.83	21.67 ± 3.06 17.33 ± 6.11	31.50 ± 5.45 29.75 ± 3.50
83.33	114.29 104.0 ± 10.32	114.29	88.00	80.00 87.48 ± 4.177	94.44
14.00 ± 1.83* 10.00 ± 1.41	14.50 ± 4.93* 7.00 ± 1.82§	27.75 ± 0.96* 15.25 ± 2.75†	46.50 ± 8.43* 20.25 ± 4.99†	35.33 ± 5.69* 25.00 ± 2.00	67.25 ± 5.85* 29.50 ± 6.19†
71.43	48.28 58.22 ± 6.88	54.95	43.55	70.75 52.72 ± 9.02	43.87

Table 2. Effect of MR16-1 on BLM-Induced Dermal Sclerosis in a Treatment Model

	Thickness (mm)		Hardness (arbitrary)		α-SMA–positive cells (cells/HPS)		Mast cells (cells/HPS)	
	1st (n = 4)	2nd (n = 3)	1st (n = 4)	2nd (n = 3)	1st (n = 4)	2nd (n = 3)	1st (n = 4)	2nd (n = 3)
PBS								
Control Ab	0.14 ± 0.02	0.12 ± 0.03	4.80 ± 0.47	6.19 ± 1.29	3.75 ± 1.50	2.33 ± 0.58	13.50 ± 1.73	19.67 ± 2.52
MR16-1	0.12 ± 0.01	0.107 ± 0.006	4.67 ± 0.47	5.68 ± 0.43	3.33 ± 0.56	2.67 ± 1.15	15.33 ± 1.15	21.00 ± 2.00
% Changes	83.64	86.49	97.22	91.78	88.88	106.78	113.58	106.78
BLM								
Control Ab	0.30 ± 0.03*	0.29 ± 0.03*	9.34 ± 1.58*	9.81 ± 1.17†	10.00 ± 2.58*	7.67 ± 0.58*	37.75 ± 2.50*	54.67 ± 8.39*
MR16-1	0.21 ± 0.05‡‖	0.18 ± 0.03§¶	5.46 ± 0.62¶	5.41 ± 0.77¶	5.50 ± 1.29¶	4.00 ± 1.00¶	27.00 ± 2.16§¶	37.00 ± 6.56‡‖
% Changes	70.00	62.50	58.46	55.12	55.00	52.17	71.52	67.68

Mean ± SD is presented. To quantify the impact of MR16-1treatment, % changes were calculated as follows: (evaluative consequences of MR16-1 treatment/that of PBS treatment) × 100 (%).
*P < 0.01 PBS+Control Ab versus BLM+Cont. Ab.
†P < 0.05 PBS+Control Ab versus BLM+Cont. Ab.
‡P < 0.05 BLM+Control Ab versus BLM+MR16-1.
§P < 0.01 PBS+MR16-1 versus BLM+MR16-1.
¶P < 0.01 BLM+Control Ab versus BLM+MR16-1
‖P < 0.05 PBS+MR16-1 versus BLM+MR16-1.
HPS, high-power field.

sense 5′-TGTCATCATACTTGGCAGGTTTCT-3′, antisense 5′-CATGGCCTTCCGTGTTCCTA-3′. Real-time PCR (40 cycles of denaturing at 92°C for 15 seconds and annealing at 60°C for 60 seconds) was run on an ABI 7000 Prism Detection System (Applied Biosystems).

Mouse IL-6 Receptor–Specific Monoclonal Antibody Treatment

Rat anti-mouse IL-6 receptor monoclonal Ab (clone MR16-1, rat $IgG_{1)}$ described previously[18] was provided by Chugai Pharmaceutical (Shizuoka, Japan). Purified rat IgG_1 (isotype-matched control Ab) (Cappel, MP Biomedicals, Solon, OH) was administered as a control. Preventive and therapeutic administration methods are discussed later. Percentage to control values were calculated as follows: (mean actual value/mean control value) × 100.

Enzyme-Linked Immunosorbent Assay of IL-6 Levels in Sera and Conditioned Media

Serum samples were obtained from mice injected with BLM or PBS for 28 days. Conditioned media were obtained from cultured primary dermal fibroblasts of wild-type and *Il-6*KO mice after 24 hours. Serum and conditioned media IL-6 level was measured by enzyme-linked immunosorbent assay using a commercial kit (R&D Systems, Minneapolis, MN) with a detection limit of 7.8 pg/mL.

Vesmeter Measurements

Skin hardness was measured using a Vesmeter.[19] Mice were sacrificed 1 day after the final injection. Skin hardness was measured three times at the injection area, avoiding the backbone of the mouse. Skin hardness was expressed as the area of the depression caused by the

Table 3. Attenuated BLM-Induced Dermal Sclerosis in *Il-6*KO Mice

	Thickness (mm)		Hardness (arbitrary)		α-SMA–positive cells (cells/HPS)		Mast cells (cells/HPS)	
	1st (n = 4)	2nd (n = 3)	1st (n = 4)	2nd (n = 3)	1st (n = 4)	2nd (n = 3)	1st (n = 4)	2nd (n = 3)
WT								
PBS	0.112 ± 0.013	0.14 ± 0.04	4.91 ± 0.38	5.46 ± 0.93	4.75 ± 1.50	8.00 ± 2.00	18.00 ± 3.16	28.33 ± 4.51
BLM	0.32 ± 0.02*	0.29 ± 0.06†	12.38 ± 0.81*	9.69 ± 0.51*	19.75 ± 5.74*	23.33 ± 6.11*	40.25 ± 2.22*	63.33 ± 9.87*
% Change	282.85	203.13	251.99	177.28	415.79	291.67	223.61	223.53
Il-6								
PBS	0.111 ± 0.010	0.12 ± 0.01	5.37 ± 0.48	5.12 ± 0.71	4.00 ± 1.41	6.67 ± 2.52	17.75 ± 2.5	29.5 ± 0.71
BLM	0.22 ± 0.03‡§	0.17 ± 0.03‡	7.14 ± 0.96‡¶	5.85 ± 0.21‡	9.50 ± 4.43‖	13.00 ± 1.73‖	22.75 ± 4.79‡	34.00 ± 7.00‖
% Change	195.71	133.81	132.87	114.21	237.50	195.00	128.17	115.25

Mean ± SD was presented. To quantify the impact of BLM treatment, % changes were calculated as follows: (evaluative consequences of BLM treatment/that of PBS treatment) × 100 (%).
*P < 0.01 WT with PBS versus WT with BLM.
†P < 0.05 WT with PBS versus WT with BLM.
‡P < 0.01 WT with BLM versus *Il-6*KO with BLM.
§P < 0.01 *Il-6*KO with PBS versus *Il-6*KO with BLM.
¶P < 0.05 *Il-6*KO with PBS versus *Il-6*KO with BLM.
‖P < 0.05 WT with BLM versus *Il-6*KO with BLM.
HPS, high-power field; WT, wild-type.

Table 4. Number of Lymph Node Cells in the Scleroderma Mouse Model

	1st experiment (total number/lymph node, × 10^7)			2nd experiment (total number/lymph node, × 10^6)		
	PBS	BLM	% Change	PBS	BLM	% Change
WT						
Control Ab	0.97 ± 0.21 (n = 3)	2.17 ± 0.31* (n = 3)	222.61	1.90 ± 0.41 (n = 4)	3.55 ± 0.21* (n = 4)	186.73
MR16-1	0.76 ± 0.02 (n = 3)	0.80 ± 0.12† (n = 3)	105.29	1.85 ± 0.18 (n = 4)	1.85 ± 0.34† (n = 4)	99.84
*Il-6*KO						
WT	0.81 ± 0.18 (n = 3)	1.53 ± 0.40‡ (n = 3)	190.03	2.36 ± 0.26 (n = 3)	3.71 ± 0.61‡ (n = 3)	157.42
*Il-6*KO	0.66 ± 0.26 (n = 3)	0.54 ± 0.09§ (n = 3)	82.73	1.97 ± 0.67 (n = 3)	2.20 ± 0.29§ (n = 3)	111.51

Mean ± SD was presented. To quantify the impact of BLM treatment, % changes were calculated as follows: (evaluative consequences of BLM treatment/that of PBS treatment) × 100 (%).
*P < 0.01 PBS+Control Ab versus BLM+Cont. Ab.
†P < 0.01 BLM+Control Ab versus BLM+MR16-1.
‡P < 0.05 PBS+Control Ab versus BLM+Cont. Ab.
§P < 0.05 BLM+Control Ab versus BLM+MR16-1.

probe divided by the pressure of the indenter in a connected computer.

Histopathological Analysis

The back skin was removed 1 day after the final injection. Skin pieces were fixed with 10% formaldehyde for 24 hours, embedded in paraffin, and sectioned at 3-μm thickness using a microtome. Sections were stained with hematoxylin and eosin (H&E). Dermal thickness (measured from the epidermal–dermal junction to dermal–fat junction) was determined at ×100 magnification at three randomly selected sites in each animal. Mast cells were identified in 3-μm deparaffinized sections stained with 1% Toluidine Blue, and mast cells were counted in 10 randomly selected sites under × 400 power using light microscopy.

Immunohistochemical Analysis of α-SMA

Sections were cut and processed as described above. For immunohistochemical analysis, sections were deparaffinized by passage through xylene and graded ethanols. Next, endogenous peroxide was blocked using 3% H_2O_2 in methanol for 5 minutes. Slides were blocked with 2% bovine serum albumin for 10 minutes, and stained with primary Ab (anti–α-SMA Ab 1:100 dilution) for 60 minutes. After washing with PBS containing 0.05% Triton, they were developed using Dako ChemMate Envision Kit/horseradish peroxidase (Dako-Cytomation) for 30 minutes, and counterstained with hematoxylin. α-SMA–positive fibroblastic cells were counted in 10 randomly selected sites under × 400 power using light microscopy.

Flow Cytometric Analysis

The skin draining LNs were assessed as a mixture to facilitate analysis. One day after the final infection, mice were sacrificed, and axillary, brachial, and inguinal LNs from each mouse were combined. Cell suspensions of LN cells were stained with antibodies against the following cell surface antigens: CD4, CD8, B220, CD11c, F4/80, and PDCA1 (BD Biosciences, San Jose, CA). Stained cells were analyzed by flow cytometry using a FACSCalibur flow cytometer (BD Biosciences).

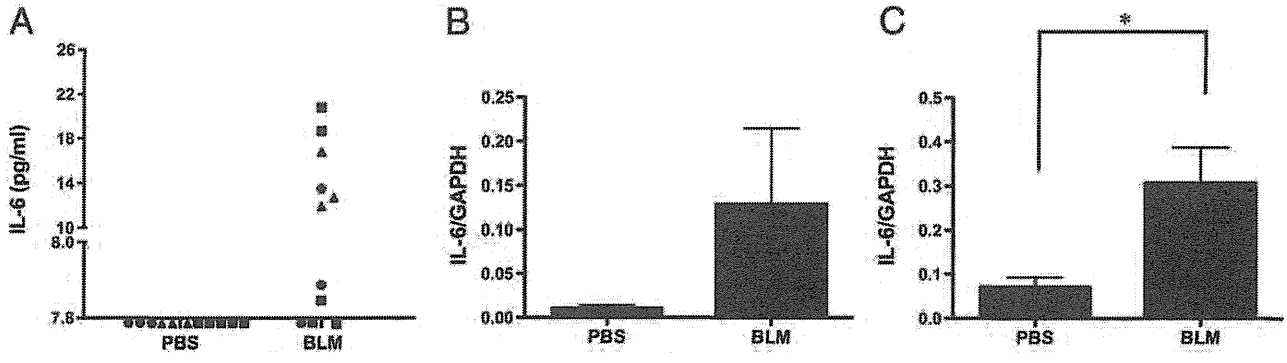

Figure 1. IL-6 production in BLM-treated C57BL/6 mice. C57BL/6 mice treated with PBS or BLM for 4 weeks. **A:** Serum samples were obtained from mice injected with 1 mg/mL BLM (100 μL/day, n = 11) or PBS (100 μL/day, n = 11) for 4 weeks. The data presented are from three experiments of three to five mice each for a total of 11 BLM-treated mice and 11 PBS-treated mice. Serum IL-6 level was measured by enzyme-linked immunosorbent assay using a kit with a detection limit of 7.8 pg/mL (R&D Systems). The mice from different experiments were gave different symbols [box (n = 5), circle (n = 3), and triangles (n = 3)]. Each symbol represents one IL-6 measurement for a single mouse, and symbols below 7.8 pg/mL indicate mice for which IL-6 was below the limit of detection. enzyme-linked immunosorbent assays were run in duplicate for all mice, with similar results. **B** and **C:** Expression of IL-6 mRNA was measured by real-time PCR. RNA was extracted from skin lesions (**B**) and cutaneous draining LNs (**C**) from C57BL/6 mice treated with PBS (n = 3) or BLM (n = 3) for 4 weeks. Data were normalized to the GAPDH internal control. Bars represent mean ± SD. *P < 0.05, unpaired t-test. Data in B and C are from one of two independent experiments that gave similar results. The IL-6/GAPDH data (mean ± SD) for skin lesions (**B**) were as follows: first experiment (n = 3), PBS: 0.011 ± 0.006, BLM: 0.129 ± 0.148 (P = 0.2391); second experiment (n = 3), PBS: 0.142 ± 0.070, BLM: 0.441 ± 0.283 (P = 0.1495). The IL-6/GAPDH data (mean ± SD) for cutaneous draining LNs (**C**) were as follows: first experiment (n = 3), PBS: 0.071 ± 0.038, BLM: 0.306 ± 0.141 (P = 0.0493), second experiment (n = 3), PBS: 0.083 ± 0.0.067, BLM: 0.430 ± 0.175 (P = 0.0321).

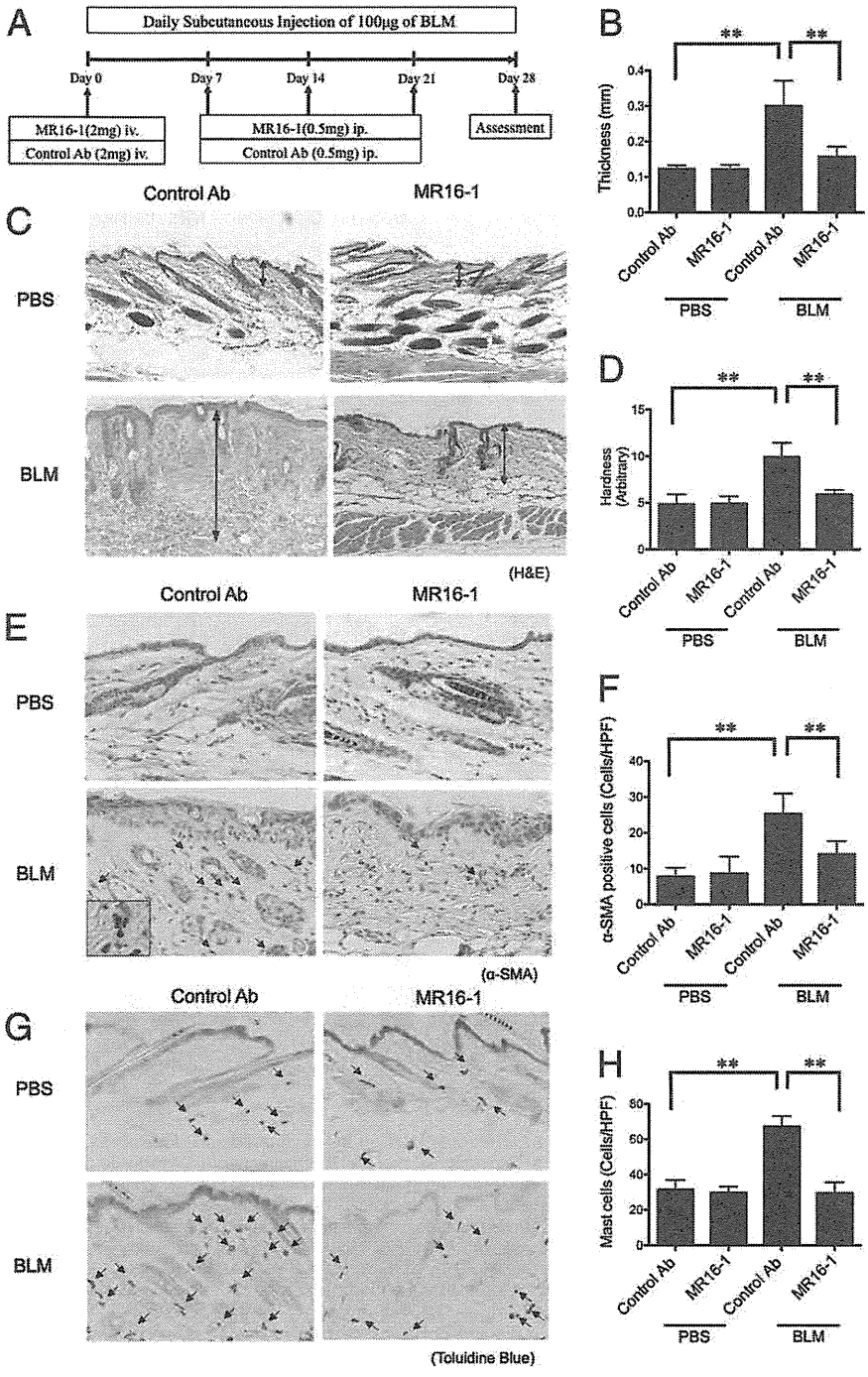

Figure 2. Effect of MR16-1 on BLM-induced dermal sclerosis in a prevention model. **A:** Experimental protocol for prevention of BLM-induced dermal sclerosis by administration of MR16-1 or control Ab to either PBS- or BLM-treated mice ($n = 4$ for each group). Histological and physical examination of the lesional skin was performed on the final day (day 28) of the protocol. **B:** Measurements of dermal thickness ($n = 4$ for each group). **C:** H&E staining of specimens derived from PBS-, or BLM-injected mice treated with MR16-1 or control Ab (original magnification, ×40). The length of each **two-headed arrow** indicates the measurement region of dermal thickness. **D:** Skin hardness measurements obtained using a Vesmeter ($n = 4$ for each group). **E:** Immunohistochemical staining for α-SMA. **Arrows** indicate α-SMA–positive fibroblasts (original magnification, ×100). **Inset** photo shows higher magnification (×200) of α-SMA–positive fibroblasts. **F:** The number of α-SMA–positive fibroblasts per high-power field (HPF, ×400) was determined by observation of 10 random grids. The value graphed is the average of the observation of 10 grids for each of the four mice in the group. **G:** Results of Toluidine Blue staining. **Arrows** indicate the metachromatically stained mast cells (original magnification, ×100). **H:** The number of mast cells per HPF (×400) was determined by observation of 10 random grids. The value graphed is the average of the observation of 10 grids for each of the four mice in the group. **C**, **D**, **F**, and **H:** Bars represent mean ± SD. $^{*}P < 0.05$, $^{**}P < 0.01$, one-way analysis of variance and Bonferroni post hoc multiple comparison. Data presented are from the third of three independent experiments with similar results presented in Table 1.

Computation Methods and Statistical Analysis

All data except change ratios are expressed as mean values ± standard deviations (SDs). To quantify the impact of MR16-1-and BLM treatment, change ratios (%) are calculated for single experiments in Table 1–4. Percent changes in Table 1 are averaged for three experiments and expressed as mean values ± standard errors (SEs). Unpaired *t*-test was used to examine the statistical value between two variable quantities. One-way analysis of variance and the Bonferroni post hoc multiple comparison procedure were used to determine the level of significance between each of three or more variable quantities.

Results

Elevated IL-6 in Mice with BLM-Induced Scleroderma

We first determined the serum concentration and mRNA expression of IL-6 in the skin and cutaneous draining LNs from mice with skin fibrosis induced by subcutaneous

BLM injection. Serum IL-6 levels were undetectable by enzyme-linked immunosorbent assay in all PBS-treated mice, and in 3 of 11 C57BL/6 mice treated with BLM. However, IL-6 was detectable, thus elevated, in 8 of 11 BLM-treated mice (Figure 1A), with a mean of 11.9 ± 5.24 pg/mL (n = 8). IL-6 mRNA expression showed a trend toward increased levels in the skin of mice treated with BLM that was not statistically significant (Figure 1B), and was significantly elevated ($P < 0.05$) in the cutaneous draining LNs of BLM-treated mice relative to PBS-treated mice (Figure 1C). These results are consistent with a role for IL-6 in the pathogenesis of scleroderma in the BLM-induced mouse model.

MR16-1 Prevents BLM-Induced Dermal Sclerosis

We next investigated whether MR16-1, a rat anti-mouse IL-6 receptor monoclonal Ab, could ameliorate the dermal thickening and skin hardening symptoms observed in BLM-treated mice. Figure 2A shows the administration schedule of preventive intervention. Dermal thickness was significantly increased at the BLM injection site of control Ab–treated mice, but nearly normal at the PBS injection site of control Ab–, or MR16-1–treated mice. Importantly, BLM-induced dermal thickening was significantly attenuated by prophylactic administration of MR16-1 (Figure 2, B and C, Table 1).

Skin hardness in the BLM-injected group that was given MR16-1 was also significantly reduced compared to the BLM-injected group that was given the control Ab. The ameliorating effect of MR16-1 on skin hardness was relatively strong compared with the effect on dermal thickness (Figure 2, B and D, Table 1).

To further examine the effects of MR16-1 treatment, the numbers of α-SMA–positive fibroblasts (termed myofibroblasts) (Figure 2, E and F, Table 1) and mast cells (Figure 2, G and H, Table 1), both key players in sclerosis of skin lesions, were evaluated. The numbers of myofibroblasts and mast cells were significantly increased in BLM-injected mice treated with control Ab relative to PBS-injected mice treated with control Ab. In BLM-injected mice treated with MR16-1, the numbers of myofibroblasts and mast cells were decreased significantly compared to the control value (BLM-injected mice treated with control Ab) (Figure 2, E to H, Table 1). These results suggest that treatment with MR16-1 might be effective during the fibrosing phase of scleroderma.

MR16-1 Improves BLM-Induced Dermal Sclerosis

Figure 3A shows the administration schedule of treatment intervention. As expected, the dermal thickness and skin hardness induced by BLM were diminished by therapeutic administration of MR16-1 compared with control Ab (Figure 3, B to D). The numbers of myofibroblasts and mast cells in lesional skin were also decreased by administration of MR16-1 compared with control Ab (Figure 3, E and F). Table 2 summarizes the data from two treatment intervention experiments. These results indicate that IL-6 may contribute to the pathogenesis of BLM-induced scleroderma and that blockade of IL-6 receptor may be a novel treatment of scleroderma.

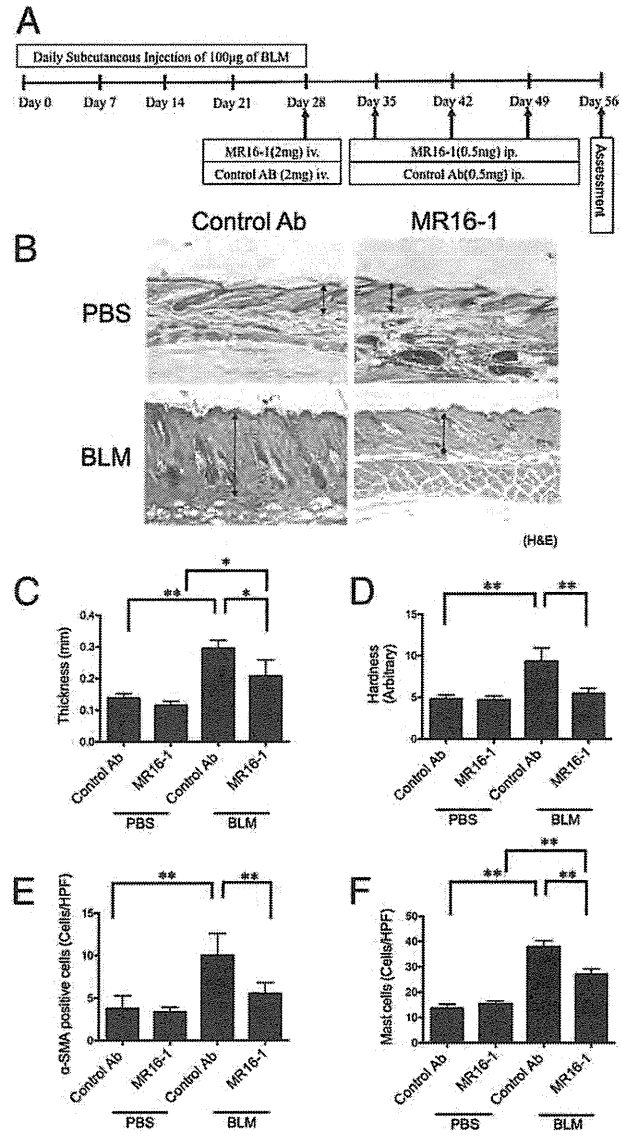

Figure 3. Effect of MR16-1 on BLM-induced dermal sclerosis in a treatment model. **A:** Experimental protocol for treatment of BLM-induced dermal sclerosis by administration of MR16-1 or control Ab to either PBS- or BLM-treated mice (n = 3~4 for each group). The effect of Ab therapy was assessed on day 56. **B:** H&E staining of specimens derived from PBS- or BLM-injected mice treated with MR16-1 or control Ab (original magnification, ×40), and measurements of dermal thickness (**C**) (the measurement region of dermal thickness was indicated with the length of each **two-headed arrow** in **B**) and skin hardness (**D**). The number of α-SMA–positive fibroblasts (**E**) and mast cells (**F**) per HPF (×400) were determined by observation of 10 random grids. The value graphed is the average of the observation of 10 grids for each of the four mice in the group. **C** to **F:** Bars represent mean ± SD. $^{*}P < 0.05$, $^{**}P < 0.01$, one-way analysis of variance and Bonferroni post hoc multiple comparison. Data presented are from the first of two independent experiments with similar results. See Table 2 for data from both experiments.

IL-6 Directly Modulates α-SMA Expression in Dermal Fibroblasts in Vitro

We next focused on whether dermal fibroblasts are a target of IL-6. Nontreated primary dermal fibroblasts from wild-type mice already express α-SMA, and stimulation

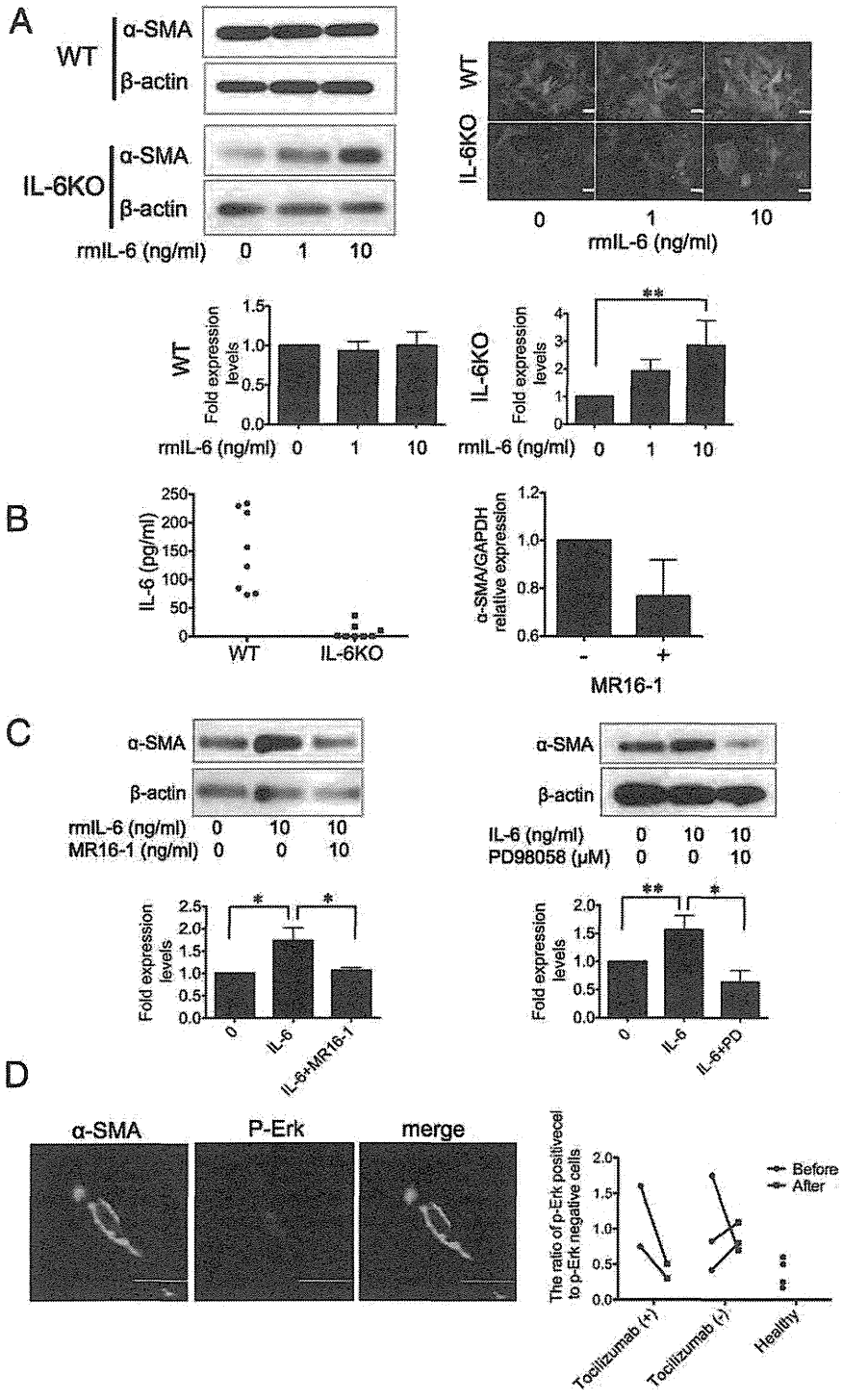

Figure 4. IL-6 induces α-SMA protein expression in cultured *Il-6*KO fibroblasts. **A:** α-SMA expression following recombinant mouse Il-6 (rmIL-6) stimulation was determined by immunofluorescent staining and Western blot analysis. α-SMA and nucleus were show in green and blue, respectively. Scale bar = 100 μm. β-Actin expression was used to determine fold changes in expression by densitometry. Cultured dermal fibroblasts from wild-type (WT) and *Il-6*KO mice were treated with 0, 1, and 10 ng/mL rmIL-6 for 24 hours. These experiments were repeated three times, and the results of densitometric analyses are presented as the fold change (mean ± SD) compared with control. $^{**}P < 0.01$, one-way analysis of variance and Bonferroni post hoc multiple comparisons. **B:** *Il-6* levels in supernatants of cultured dermal fibroblasts from WT and *Il-6*KO mice (**left**) after 24 hours. MR16-1 treatment decreased α-SMA mRNA expression in cultured primary WT dermal fibroblasts (**right**). **C:** MR16-1 and ERK inhibitor, PD98058, attenuated rmIL-6–induced α-SMA protein expression in cultured *Il-6*KO fibroblasts. β-Actin expression was used to determine fold changes in expression by densitometry. These experiments were performed three times, and the results of densitometric analyses are presented as the fold change (mean ± SD) compared with control. $^{**}P < 0.01$, $^{*}P < 0.05$, one-way analysis of variance and Bonferroni post hoc multiple comparisons. **D:** Immunofluorescent staining for phosphorylated ERK (p-ERK, red) and α-SMA (green) in lesional skin derived from two tocilizumab-treated patients with scleroderma. A representative image of p-ERK$^+$, α-SMA$^+$ fibroblasts (original magnification, ×1200) is shown. The number of p-ERK–positive α-SMA–positive fibroblasts per HPF (×400) was determined by observation of 10 random grids. Scale bar = 50 μm. The ratio of p-ERK–positive fibroblasts was calculated as follows: the number of p-ERK$^+$, α-SMA$^+$ fibroblasts/the number of p-ERK$^-$, α-SMA$^+$ fibroblasts.

with exogenous recombinant mouse IL-6 (rmIL-6) did not alter α-SMA expression (Figure 4A). Further, highly expressed levels of endogenous IL-6 from nontreated cultured primary wild-type dermal fibroblasts and decreased levels of α-SMA mRNA expression after MR16 treatment indicated that hyporesponsiveness of cultured primary wild-type dermal fibroblasts to exogenous IL-6 was presumably due to the autocrine regulation of α-SMA by IL-6 (Figure 4B). Thus, we switched to primary *Il-6*KO mouse–derived fibroblasts and evaluated α-SMA expression using immunofluorescent staining and Western blot analysis. Low-level expression was observed in nontreated *Il-6*KO dermal fibroblasts, but stimulation with 1 or 10 ng/mL of rmIL-6 induced α-SMA expression in a dose-dependent manner (Figure 4A). α-SMA induction by rmIL-6 was inhibited by 10 ng/mL MR16-1 and also by the ERK1/2 inhibitor PD98059 (Figure 4C).

These results led us to examine whether the positive effects of clinical treatment with tocilizumab might correlate with reduced numbers of ERK-activated α-SMA–pos-

itive dermal fibroblasts in lesional skin of scleroderma patients. The number of Erk-activated α-SMA–positive cells in lesional skin in scleroderma patients treated with tocilizumab for 6 months was reduced to a similar level as in healthy skin, whereas the number in scleroderma patients treated with 10 mg/day of prednisolone for 6 months without tocilizumab was diminished in one patient and increased in two patients (Figure 4D).

Attenuated BLM-Induces Dermal Sclerosis in Il-6KO Mice

To investigate the role of IL-6 in BLM-induced dermal sclerosis, *Il-6*KO mice received subcutaneous injection of BLM or PBS for 4 weeks, and histological and physical examination of the lesional skin was performed (Figure 5A, Table 3). We found that BLM-induced dermal sclerosis in *Il-6*KO mice was attenuated compared with that in wild-type mice. Lack of visible changes in the skin between PBS-treated *Il-6*KO mice and PBS-treated wild-type mice indicated that IL-6 might not be involved in dermal homeostasis (Figure 5A). After 4 weeks of BLM treatment, dermal thickness and skin hardness in *Il-6*KO mice were significantly attenuated compared to wild-type mice (Figure 5A). The numbers of α-SMA–positive cells and mast cells in BLM-treated *Il-6*KO mice were significantly reduced compared to BLM-treated wild-type mice (Figure 5B). Table 3 summarizes the data from two experiments. These results indicate that IL-6 is likely to play an important role in promoting the fibrogenic responses elicited by BLM treatment.

Enlarged Draining LNs Are Reduced in Size by a Block of IL-6 in the Mouse Model and in a Patient with Scleroderma

We found that cutaneous draining LNs were visibly enlarged by BLM treatment in the scleroderma model mice, but not by PBS treatment (Figure 6A, Table 4). The total LN cell count per LN in control Ab–treated BLM-injected mice was significantly increased compared with control Ab–treated PBS-injected mice, and decreased by administration of MR16-1 to BLM-injected mice. Although it was only from a single experiment with a small number of mice, the weight per LN also showed similar findings to the results of the total LN cell count per LN. However, no histological differences were observed between LNs from BLM- and PBS-injected control Ab–treated mice (Figure 6A). Detailed cell fractionation analysis (using cell-surface antigens CD4, CD8, B220, CD11c, F4/80, and PDCA1) of cells isolated from the draining LNs revealed that the ratio of $PDCA1^{+}CD11c^{+}$ double-positive cells [plasmacytoid dendritic cells (pDCs)] was significantly increased in the draining LNs of prophylactically MR16-1–treated model mice (Figure 6B). Further, draining LNs were not grossly enlarged in BLM-treated *Il-6*KO mice (Figure 6C, Table 4), consistent with weight and total cell count per LN measurements in the normal range (Figure 6C).

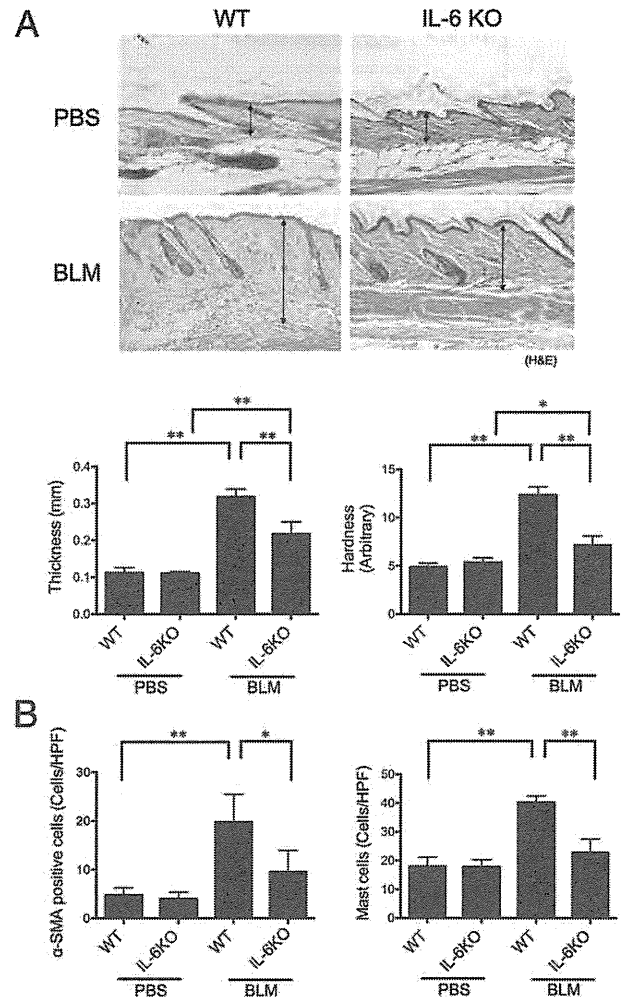

Figure 5. Attenuated BLM-induced dermal sclerosis in *Il-6*KO mice. **A:** H&E staining of skin specimen derived from PBS- and BLM-treated wild-type (WT) and *Il-6*KO mice (original magnification × 40), and measurements of dermal thickness (**lower left panel**) and skin hardness (**lower right panel**). The length of the **two-headed arrows** indicates the measurement region of dermal thickness. **B:** The number of α-SMA–positive fibroblasts (**left panel**) and mast cells (**right panel**) per HPF (×400) was determined by observation of 10 random grids. **A** and **B:** Bars represent mean ± SD ($n = 4$ for each group). $^{*}P < 0.05$, $^{**}P < 0.01$, one-way analysis of variance and Bonferroni post hoc multiple comparison. Data presented are from the first of two independent experiments that yielded similar results, and Table 3 presents data from both experiments.

We then examined whether LNs were enlarged in a patient with scleroderma, and found swelling of axillary LNs on computed tomography scan (Figure 6D), which was not detected after the administration of tocilizumab (Figure 6D).

Discussion

Our study demonstrates the critical role of IL-6 in dermal sclerosis. Blockade of IL-6 receptor with MR16-1 in the BLM-treated mice alleviates dermal sclerosis. This report also addresses outstanding problems in scleroderma pathogenesis, including the target of IL-6.

The source(s) of the elevated IL-6 in the sera of patients with scleroderma are still unclear. Several lines of

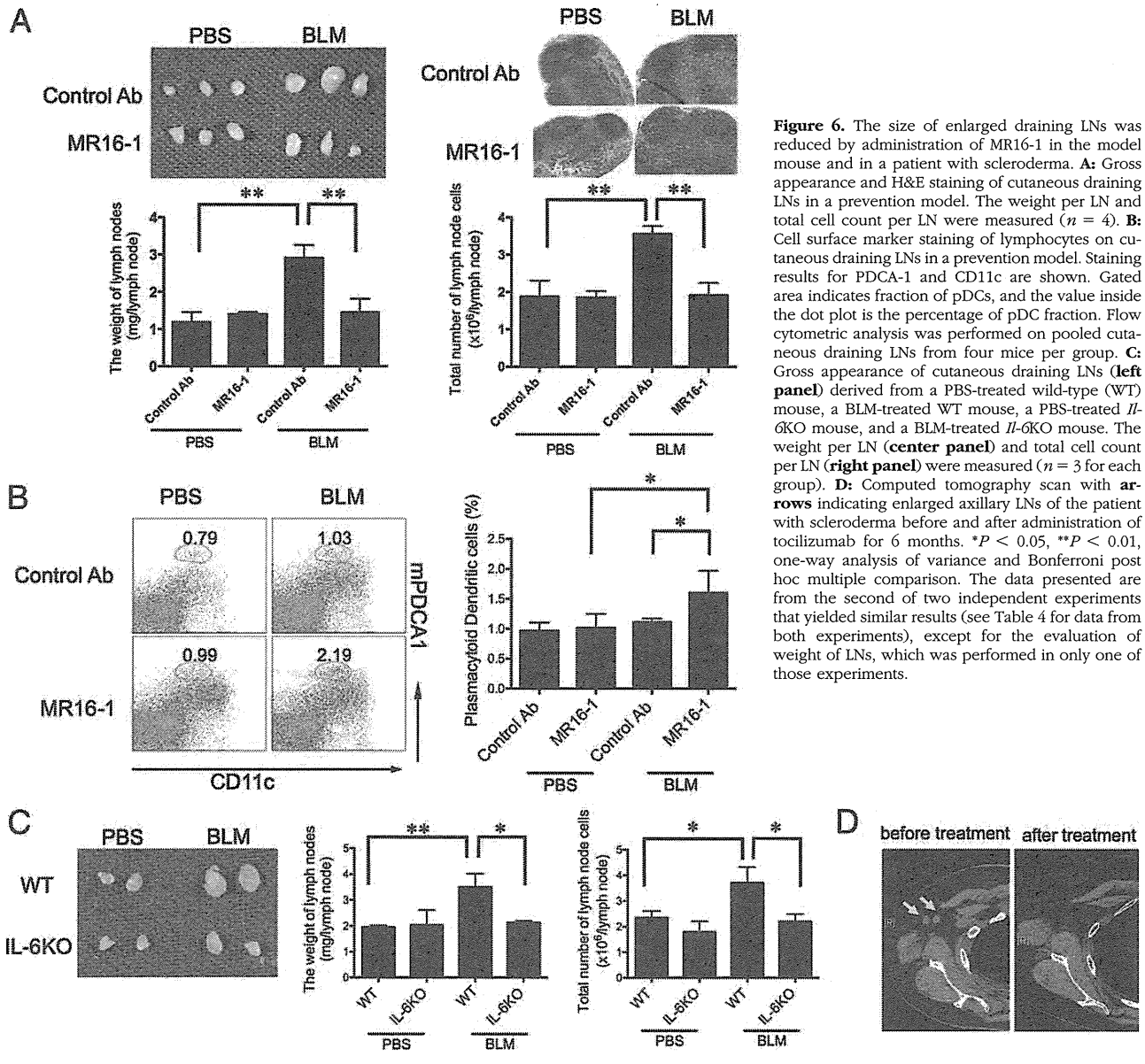

Figure 6. The size of enlarged draining LNs was reduced by administration of MR16-1 in the model mouse and in a patient with scleroderma. **A:** Gross appearance and H&E staining of cutaneous draining LNs in a prevention model. The weight per LN and total cell count per LN were measured ($n = 4$). **B:** Cell surface marker staining of lymphocytes on cutaneous draining LNs in a prevention model. Staining results for PDCA-1 and CD11c are shown. Gated area indicates fraction of pDCs, and the value inside the dot plot is the percentage of pDC fraction. Flow cytometric analysis was performed on pooled cutaneous draining LNs from four mice per group. **C:** Gross appearance of cutaneous draining LNs (**left panel**) derived from a PBS-treated wild-type (WT) mouse, a BLM-treated WT mouse, a PBS-treated *Il-6*KO mouse, and a BLM-treated *Il-6*KO mouse. The weight per LN (**center panel**) and total cell count per LN (**right panel**) were measured ($n = 3$ for each group). **D:** Computed tomography scan with **arrows** indicating enlarged axillary LNs of the patient with scleroderma before and after administration of tocilizumab for 6 months. $^{*}P < 0.05$, $^{**}P < 0.01$, one-way analysis of variance and Bonferroni post hoc multiple comparison. The data presented are from the second of two independent experiments that yielded similar results (see Table 4 for data from both experiments), except for the evaluation of weight of LNs, which was performed in only one of those experiments.

evidence suggest peripheral blood mononuclear cells are a source. The supernatant concentration of IL-6 was reported to be statistically significantly elevated in peripheral blood mononuclear cells[6,20,21] and in T-cell lines[6] derived from patients with systemic sclerosis compared with healthy controls. It also has been reported that experimentally activated B cells might be prone to produce IL-6.[22,23] Other lines of evidence implicate dermal fibroblasts as an important source of IL-6.[13,24–28] In this report, although the expression of IL-6 mRNA in both lesional skin and draining LNs was increased by BLM treatment, the specific cell type producing IL-6 was not identified. Further studies are required to clarify the source(s) of IL-6.

How does secreted IL-6 contribute to the pathogenesis of scleroderma? IL-6 might modulate α-SMA expression in dermal fibroblasts and induce myofibroblasts, which are known to produce collagen[29] and induce sclerotic change.[11,30] We observed IL-6 effects on α-SMA expression from *Il-6*KO dermal fibroblasts *in vitro* in this study (Figure 4A). Unexpectedly, nontreated cultured wild-type dermal fibroblasts strongly expressed α-SMA (Figure 4A), the expression of which was not affected by exogenous IL-6, whereas MR16-1 treatment decreased the expression of α-SMA mRNA (Figure 4, A and B). Therefore, continuous autocrine production of IL-6 by wild-type cultured dermal fibroblasts might increase the threshold for reactivity to IL-6.

Furthermore, in both prevention and treatment protocols with MR16-1, the reduction in dermal sclerosis was accompanied by decreasing numbers of myofibroblasts, which are known as activated fibroblasts with strong fibrogenic property. The absence of myofibroblasts at the BLM injection site of *Il-6*KO mice indicates that IL-6–induced dermal sclerosis occurs via induction of myofibroblasts. Thus, we hypothesize that MR16-1 and tocilizumab have favorable effects on scleroderma via prevention of fibroblast activation. Administration of tocili-

zumab to scleroderma patients exhibited ameliorating effects of skin sclerosis,[15] and seemed to reduce the number of Erk-activated α-SMA–positive fibroblast in lesional skin (Figure 4D). These findings were inconclusive because of the number of cases, and further studies were required.

Another finding was reduction of LN swelling by MR16-1 treatment in mice in the BLM-induced model of scleroderma. We could not determine whether the LN swelling associated with BLM treatment was a cause or effect of BLM-induced skin sclerosis. Examination of the differential ratios of leukocytes, such as T cells, B cells, and macrophages, did not give any insight, as these were not altered after 4 weeks of BLM injection (data not shown). However, there was a slight, but significant, increase in the numbers of cells double-positive for PDCA-1^+CD11c^+ (Figure 6D) or $B220^+CD11c^+$ (data not shown) in the draining LNs of MR16-1–treated mice relative to control Ab–treated mice in the prevention model. This suggests that IL-6 might affect pDC numbers in the LNs. LN swelling is not a well-known symptom in scleroderma, and only a few articles describe LN findings in scleroderma.[31] We should keep an eye on such symptoms.

Recent studies have indicated that pDCs may promote scleroderma via secretion of type 1 interferon,[32] and induction of type 1 interferon was found by anti-topoisomerase antibody-containing serum, but not by anti-centromere antibody.[32,33] However, other data suggest MHC class II–restricted antigen presentation by pDCs might inhibit T-cell–mediated autoimmunity via selective expansion of Ag-specific natural regulatory T cells.[34] Because MHC class II–restricted proliferation of $CD4^+$ T cells had been previously thought to contribute to the pathogenesis of scleroderma,[35] one could speculate that an increased ratio of pDCs might prevent skin sclerosis via regulating peripheral tolerance. However, it is clear that the function of pDCs in pathogenesis of scleroderma is complex and needs further study.

The clear positive effects of IL-6 inhibition in mouse models with scleroderma indicate that further study of IL-6–secreting cells, effectors, and signaling in scleroderma holds great promise for the development of therapies for scleroderma, as well as for other diseases in which IL-6 can play a pivotal role.

Acknowledgments

We thank Prof. Junji Takeda (Osaka University) for expert comments and Dr. Toshiaki Hanafusa, Kenjyu Nishida, and Han Fu for technical assistance.

References

1. Preliminary criteria for the classification of systemic sclerosis (scleroderma). Subcommittee for scleroderma criteria of the American Rheumatism Association Diagnostic and Therapeutic Criteria Committee. Arthritis Rheum 1980, 23:581–590
2. Needleman BW, Wigley FM, Stair RW: Interleukin-1, interleukin-2, interleukin-4, interleukin-6, tumor necrosis factor alpha, and interferon-gamma levels in sera from patients with scleroderma. Arthritis Rheum 1992, 35:67–72
3. Hebbar M, Gillot JM, Hachulla E, Lassalle P, Hatron PY, Devulder B, Janin A: Early expression of E-selectin, tumor necrosis factor alpha, and mast cell infiltration in the salivary glands of patients with systemic sclerosis. Arthritis Rheum 1996, 39:1161–1165
4. Terao M, Murota H, Kitaba S, Katayama I: Tumor necrosis factor-alpha processing inhibitor-1 inhibits skin fibrosis in a bleomycin-induced murine model of scleroderma. Exp Dermatol 2009, 19:38–43
5. Murota H, Hamasaki Y, Nakashima T, Yamamoto K, Katayama I, Matsuyama T: Disruption of tumor necrosis factor receptor p55 impairs collagen turnover in experimentally induced sclerodermic skin fibroblasts. Arthritis Rheum 2003, 48:1117–1125
6. Scala E, Pallotta S, Frezzolini A, Abeni D, Barbieri C, Sampogna F, De Pita O, Puddu P, Paganelli R, Russo G: Cytokine and chemokine levels in systemic sclerosis: relationship with cutaneous and internal organ involvement. Clin Exp Immunol 2004, 138:540–546
7. Yamamoto T, Takagawa S, Katayama I, Yamazaki K, Hamazaki Y, Shinkai H, Nishioka K: Animal model of sclerotic skin. I: local injections of bleomycin induce sclerotic skin mimicking scleroderma, J Invest Dermatol 1999, 112:456–462
8. Yamamoto T, Takagawa S, Katayama I, Nishioka K: Anti-sclerotic effect of transforming growth factor-beta antibody in a mouse model of bleomycin-induced scleroderma. Clin Immunol 1999, 92:6–13
9. Kuwana M, Medsger TA Jr., Wright TM: Analysis of soluble and cell surface factors regulating anti-DNA topoisomerase I autoantibody production demonstrates synergy between Th1 and Th2 autoreactive T cells. J Immunol 2000, 164:6138–6146
10. Kishimoto T: The biology of interleukin-6. Blood 1989, 74:1–10
11. Gallucci RM, Lee EG, Tomasek JJ: IL-6 modulates alpha-smooth muscle actin expression in dermal fibroblasts from IL-6-deficient mice. J Invest Dermatol 2006, 126:561–568
12. Duncan MR, Berman B: Stimulation of collagen and glycosaminoglycan production in cultured human adult dermal fibroblasts by recombinant human interleukin 6. J Invest Dermatol 1991, 97:686–692
13. Kawaguchi Y, Hara M, Wright TM: Endogenous IL-1alpha from systemic sclerosis fibroblasts induces IL-6 and PDGF-A. J Clin Invest 1999, 103:1253–1260
14. Nishimoto N, Kishimoto T: Interleukin 6: from bench to bedside. Nat Clin Pract Rheumatol 2006, 2:619–626
15. Shima Y, Kuwahara Y, Murota H, Kawai M, Hirano T, Arimitsu J. Narazaki M, Hagihara K, Ogata A, Katayama I, Kawase I, Kishimoto T, Tanaka T: The skin of patients with systemic sclerosis softened during the treatment with anti-IL-6 receptor antibody tocilizumab. Rheumatology 2010, 49:2408–12
16. Gallucci RM, Sloan DK, Heck JM, Murray AR, O'Dell SJ: Interleukin 6 indirectly induces keratinocyte migration. J Invest Dermatol 2004, 122:764–772
17. Kopf M, Baumann H, Freer G, Freudenberg M, Lamers M, Kishimoto T, Zinkernagel R, Bluethmann H, Kohler G: Impaired immune and acute-phase responses in interleukin-6-deficient mice. Nature 1994, 368:339–342
18. Takagi N, Mihara M, Moriya Y, Nishimoto N, Yoshizaki K, Kishimoto T, Takeda Y, Ohsugi Y: Blockage of interleukin-6 receptor ameliorates joint disease in murine collagen-induced arthritis. Arthritis Rheum 1998, 41:2117–2121
19. Kuwahara Y, Shima Y, Shirayama D, Kawai M, Hagihara K, Hirano T, Arimitsu J, Ogata A, Tanaka T, Kawase I: Quantification of hardness, elasticity and viscosity of the skin of patients with systemic sclerosis using a novel sensing device (Vesmeter): a proposal for a new outcome measurement procedure. Rheumatology (Oxford) 2008, 47: 1018–1024
20. Hasegawa M, Sato S, Ihn H, Takehara K: Enhanced production of interleukin-6 (IL-6), oncostatin M and soluble IL-6 receptor by cultured peripheral blood mononuclear cells from patients with systemic sclerosis. Rheumatology (Oxford) 1999, 38:612–617
21. Crestani B, Seta N, De Bandt M, Soler P, Rolland C, Dehoux M, Boutten A, Dombret MC, Palazzo E, Kahn MF, et al.: Interleukin 6 secretion by monocytes and alveolar macrophages in systemic sclerosis with lung involvement. Am J Respir Crit Care Med 1994, 149: 1260–1265
22. Saito E, Fujimoto M, Hasegawa M, Komura K, Hamaguchi Y, Kaburagi Y, Nagaoka T, Takehara K, Tedder TF, Sato S: CD19-dependent B lymphocyte signaling thresholds influence skin fibrosis and

autoimmunity in the tight-skin mouse. J Clin Invest 2002, 109:1453–1462
23. Matsushita T, Hasegawa M, Yanaba K, Kodera M, Takehara K, Sato S: Elevated serum BAFF levels in patients with systemic sclerosis: enhanced BAFF signaling in systemic sclerosis B lymphocytes. Arthritis Rheum 2006, 54:192–201
24. Takemura H, Suzuki H, Fujisawa H, Yuhara T, Akama T, Yamane K, Kashiwagi H: Enhanced interleukin 6 production by cultured fibroblasts from patients with systemic sclerosis in response to platelet derived growth factor. J Rheumatol 1998, 25:1534–1539
25. Kawaguchi Y, Nishimagi E, Tochimoto A, Kawamoto M, Katsumata Y, Soejima M, Kanno T, Kamatani N, Hara M: Intracellular IL-1alpha-binding proteins contribute to biological functions of endogenous IL-1alpha in systemic sclerosis fibroblasts, Proc Natl Acad Sci U S A 2006, 103:14501–14506
26. Fukasawa C, Kawaguchi Y, Harigai M, Sugiura T, Takagi K, Kawamoto M, Hara M, Kamatani N: Increased CD40 expression in skin fibroblasts from patients with systemic sclerosis (SSc): role of CD40-CD154 in the phenotype of SSc fibroblasts. Eur J Immunol 2003, 33:2792–2800
27. Kadono T, Kikuchi K, Ihn H, Takehara K, Tamaki K: Increased production of interleukin 6 and interleukin 8 in scleroderma fibroblasts. J Rheumatol 1998, 25:296–301
28. Koch AE, Kronfeld-Harrington LB, Szekanecz Z, Cho MM, Haines GK, Harlow LA, Strieter RM, Kunkel SL, Massa MC, Barr WG, Jimenez SA: In situ expression of cytokines and cellular adhesion molecules in the skin of patients with systemic sclerosis. Their role in early and late disease. Pathobiology 1993, 61:239–246
29. Wynn TA: Cellular and molecular mechanisms of fibrosis. J Pathol 2008, 214:199–210
30. Kirk TZ, Mark ME, Chua CC, Chua BH, Mayes MD: Myofibroblasts from scleroderma skin synthesize elevated levels of collagen and tissue inhibitor of metalloproteinase (TIMP-1) with two forms of TIMP-1. J Biol Chem 1995, 270:3423–3428
31. Ofstad E: Scleroderma (progressive systemic sclerosis). A case involving polyneuritis and swelling of the lymph nodes. Acta Rheumatol Scand 1960, 6:65–75
32. Eloranta ML, Franck-Larsson K, Lovgren T, Kalamajski S, Ronnblom A, Rubin K, Alm GV, Ronnblom L: Type I interferon system activation and association with disease manifestations in systemic sclerosis. Ann Rheum Dis 2010, 69:1396–1402
33. Kim D, Peck A, Santer D, Patole P, Schwartz SM, Molitor JA, Arnett FC, Elkon KB: Induction of interferon-alpha by scleroderma sera containing autoantibodies to topoisomerase I: association of higher interferon-alpha activity with lung fibrosis. Arthritis Rheum 2008, 58: 2163–2173
34. Irla M, Kupfer N, Suter T, Lissilaa R, Benkhoucha M, Skupsky J, Lalive PH, Fontana A, Reith W, Hugues S: MHC class II-restricted antigen presentation by plasmacytoid dendritic cells inhibits T cell-mediated autoimmunity. J Exp Med 2010, 207:1891–1905
35. Kuwana M, Medsger TA Jr., Wright TM: T cell proliferative response induced by DNA topoisomerase I in patients with systemic sclerosis and healthy donors. J Clin Invest 1995, 96:586–596